

COMPLETE

up to Fall 2011

Joao **Alves**

Héctor **Arce**

Chris **Beaumont***

Michelle **Borkin***

Paola **Caselli**

James **Di Francesco**

Jonathan **Foster***

Alyssa **Goodman** (PI)

Mark **Heyer**

Doug **Johnstone**

Jens **Kauffmann**

Helen **Kirk***

Di **Li**

Jaime **Pineda***

Naomi **Ridge**

Erik **Rosolowsky**

Scott **Schnee***

Rahul **Shetty**

Mario **Tafalla**

**=COMPLETE Ph.D.*

Completely

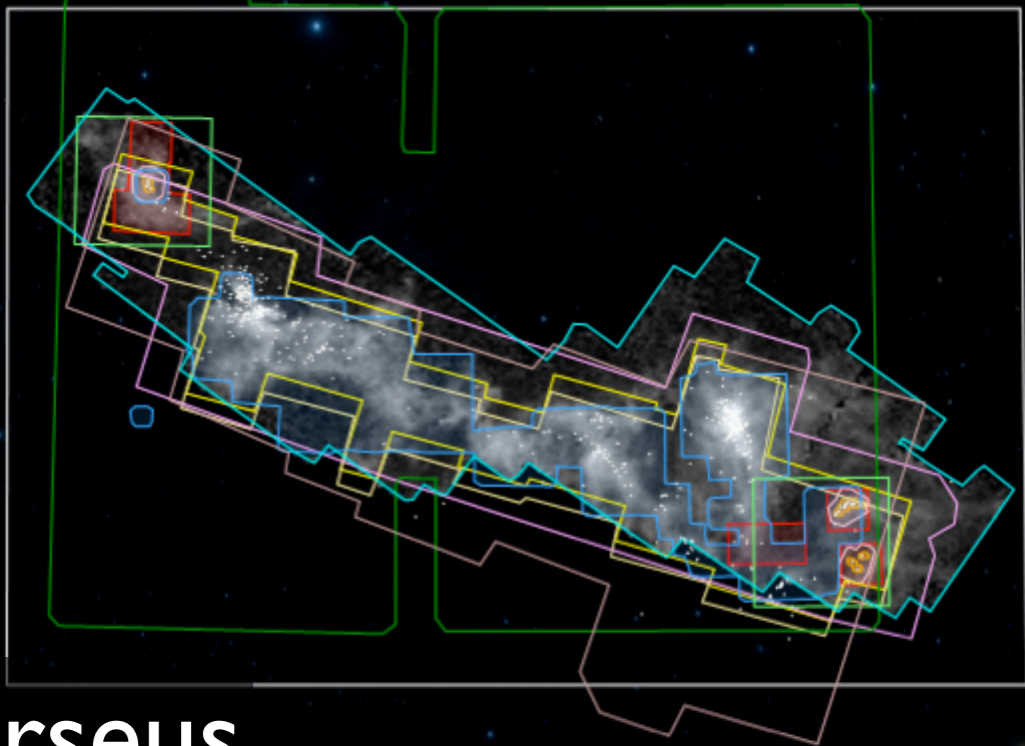
COMPLETE

Alyssa Goodman,

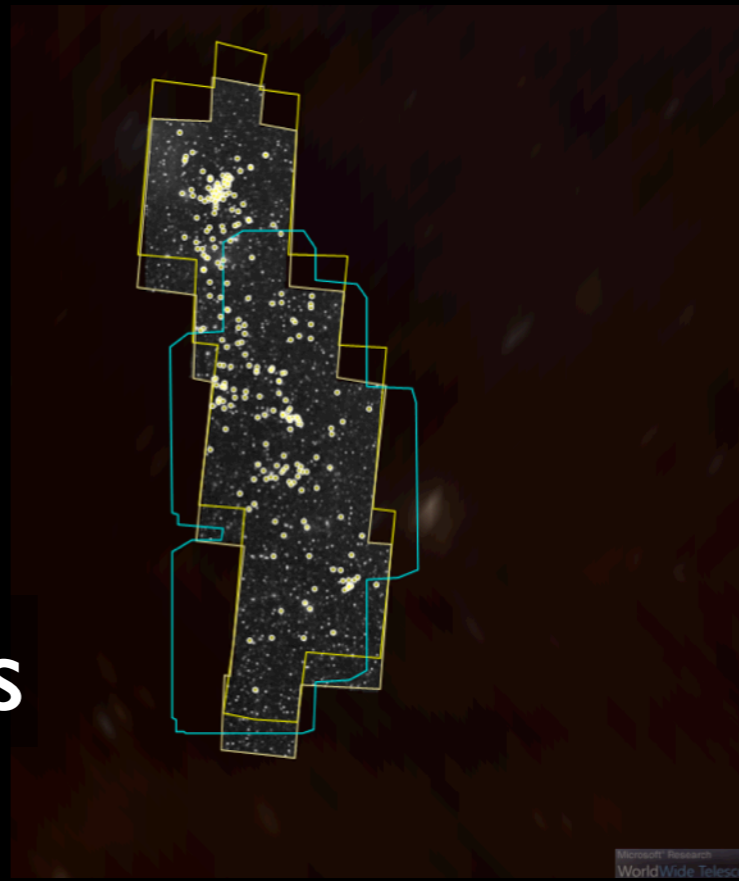
Harvard-Smithsonian Center for Astrophysics

Microsoft Research
WorldWide Telescope

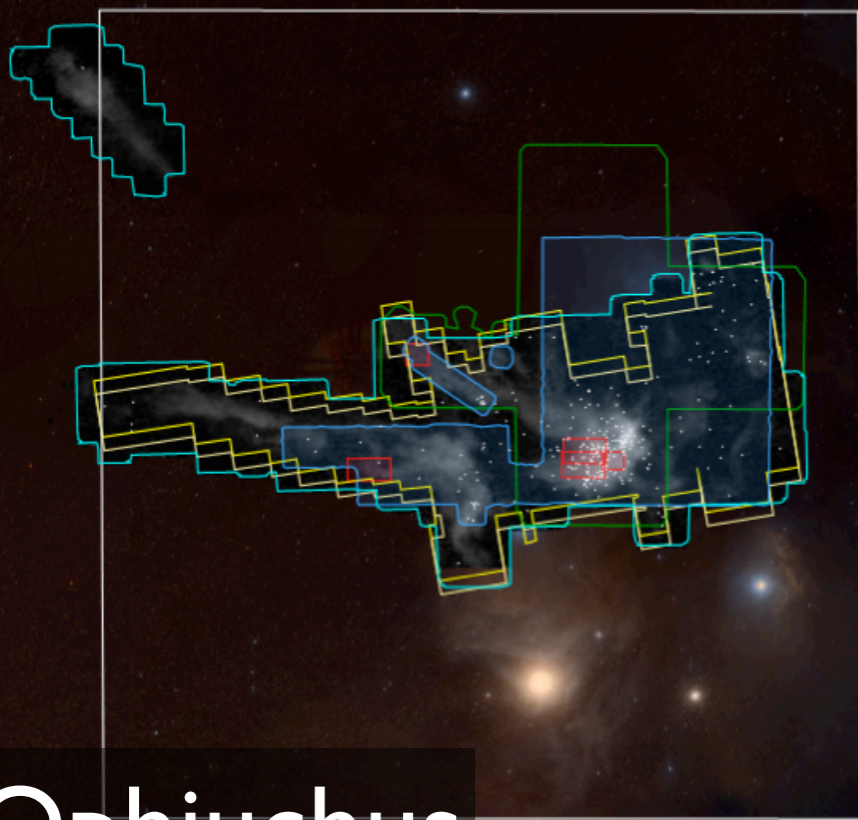
*+many thanks to special friends of COMPLETE: Hope **Chen**, Michael **Halle**, Marco **Lombardi**, Phil **Myers**, Stella **Offner**, Tom **Robitaille**, **c2d** Team, co-authors, undergrad interns...*



Perseus



Serpens



Ophiuchus

Microsoft Research
WorldWide Telescope

Microsoft Research
WorldWide Telescope

COMPLETE

The COordinated Molecular Probe Line Extinction Thermal Emission
Survey of Star-Forming Regions



www.cfa.harvard.edu/COMPLETE
tinyurl.com/completepapers

Microsoft Research
WorldWide Telescope






COMPLETE

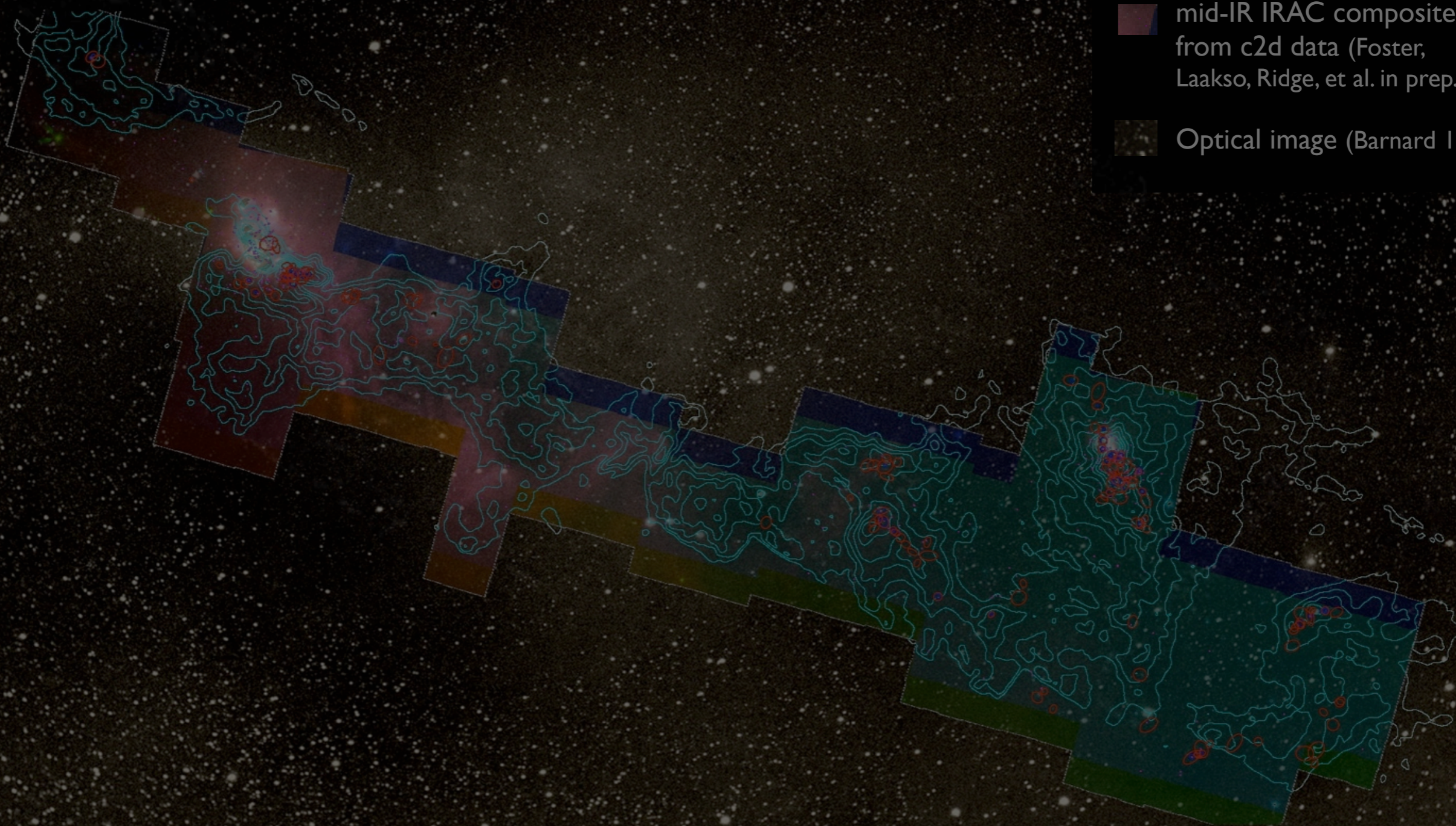
The “**C**Oordinated
Molecular **P**robe **L**ine
Exinction
Thermal **E**mission”

Survey of Star-Forming Regions

COMPLETE Perseus

Image size: 1305 x 733
VL: 63 WW: 127

-  mm peak (Enoch et al. 2006)
-  sub-mm peak (Hatchell et al. 2005, Kirk et al. 2006)
-  ^{13}CO (Ridge et al. 2006)
-  mid-IR IRAC composite from c2d data (Foster, Laakso, Ridge, et al. in prep.)
-  Optical image (Barnard 1927)



m: 17249
Zoom: 227% Angle: 0

Pineda	2011	Expanded Very Large Array Observations of the Barnard 5 Star-forming Core: Embedded Filaments Revealed
Goodman	2011	A Guide to Comparisons of Star Formation Simulations with Observations
Arce	2011	A Bubbling Nearby Molecular Cloud: COMPLETE Shells in Perseus
Shetty	2010	The Effect of Projection on Derived Mass-Size and Linewidth-Size Relationships
Pineda	2010	Direct Observation of a Sharp Transition to Coherence in Dense Cores
Kirk	2010	The Dynamics of Dense Cores in the Perseus Molecular Cloud. II. The Relationship Between Dense Cores and the Cloud
Kauffmann	2010	The Mass-Size Relation from Clouds to Cores. I. A New Probe of Structure in Molecular Clouds
Kauffmann	2010	The Mass-size Relation from Clouds to Cores. II. Solar Neighborhood Clouds
Johnstone	2010	Dense Gas Tracers in Perseus: Relating the N ₂ H ⁺ , NH ₃ , and Dust Continuum Properties of Pre- and Protostellar Cores
Heiderman	2010	The Star Formation Rate and Gas Surface Density Relation in the Milky Way: Implications for Extragalactic Studies
Arce	2010	The COMPLETE Survey of Outflows in Perseus
Shetty	2009	The Effect of Line-of-Sight Temperature Variation and Noise on Dust Continuum Observations
Shetty	2009	The Effect of Noise on the Dust Temperature-Spectral Index Correlation
Schnee	2009	The Gas Temperature of Starless Cores in Perseus
Pineda	2009	The Perils of Clumpfind: The Mass Spectrum of Substructures in Molecular Clouds
Kirk	2009	The Interplay of Turbulence and Magnetic Fields in Star-Forming Regions: Simulations and Observations
Goodman	2009	A role for self-gravity at multiple length scales in the process of star formation
Goodman	2009	The "True" Column Density Distribution in Star-Forming Molecular Clouds
Foster	2009	Dense Cores in Perseus: The Influence of Stellar Content and Cluster Environment
Schnee	2008	Dust Emission from the Perseus Molecular Cloud
Rosolowsky	2008	Structural Analysis of Molecular Clouds: Dendrograms
Rosolowsky	2008	An Ammonia Spectral Atlas of Dense Cores in Perseus
Pineda	2008	CO Isotopologues in the Perseus Molecular Cloud Complex: the X-factor and Regional Variations
Jørgensen	2008	Current Star Formation in the Ophiuchus and Perseus Molecular Clouds: Constraints and Comparisons from Unbiased Submillimeter and Mid-Infrared Surveys. II
Foster	2008	Hunting Galaxies to (and for) Extinction
Kirk	2007	Dynamics of Dense Cores in the Perseus Molecular Cloud
Kirk	2007	Erratum: "The Large- and Small-Scale Structures of Dust in the Star-forming Perseus Molecular Cloud" (ApJ, 646, 1009 [2006])
Jørgensen	2007	Current Star Formation in the Perseus Molecular Cloud: Constraints from Unbiased Submillimeter and Mid-Infrared Surveys
Schnee	2006	Estimating the Column Density in Molecular Clouds with Far-Infrared and Submillimeter Emission Maps
Ridge	2006	The COMPLETE Nature of the Warm Dust Shell in Perseus
Ridge	2006	The COMPLETE Survey of Star-Forming Regions: Phase I Data
Kirk	2006	The Large- and Small-Scale Structures of Dust in the Star-forming Perseus Molecular Cloud
Foster	2006	Cloudshine: New Light on Dark Clouds
Schnee	2005	A COMPLETE Look at the Use of IRAS Emission Maps to Estimate Extinction and Dust Temperature
Johnstone	2004	An Extinction Threshold for Protostellar Cores in Ophiuchus
Goodman	2004	The COMPLETE Survey of Star-Forming Regions on its Second Birthday

I will not do this to you...

YELLOW = something I didn't
know about or appreciate
before **COMPLETE**

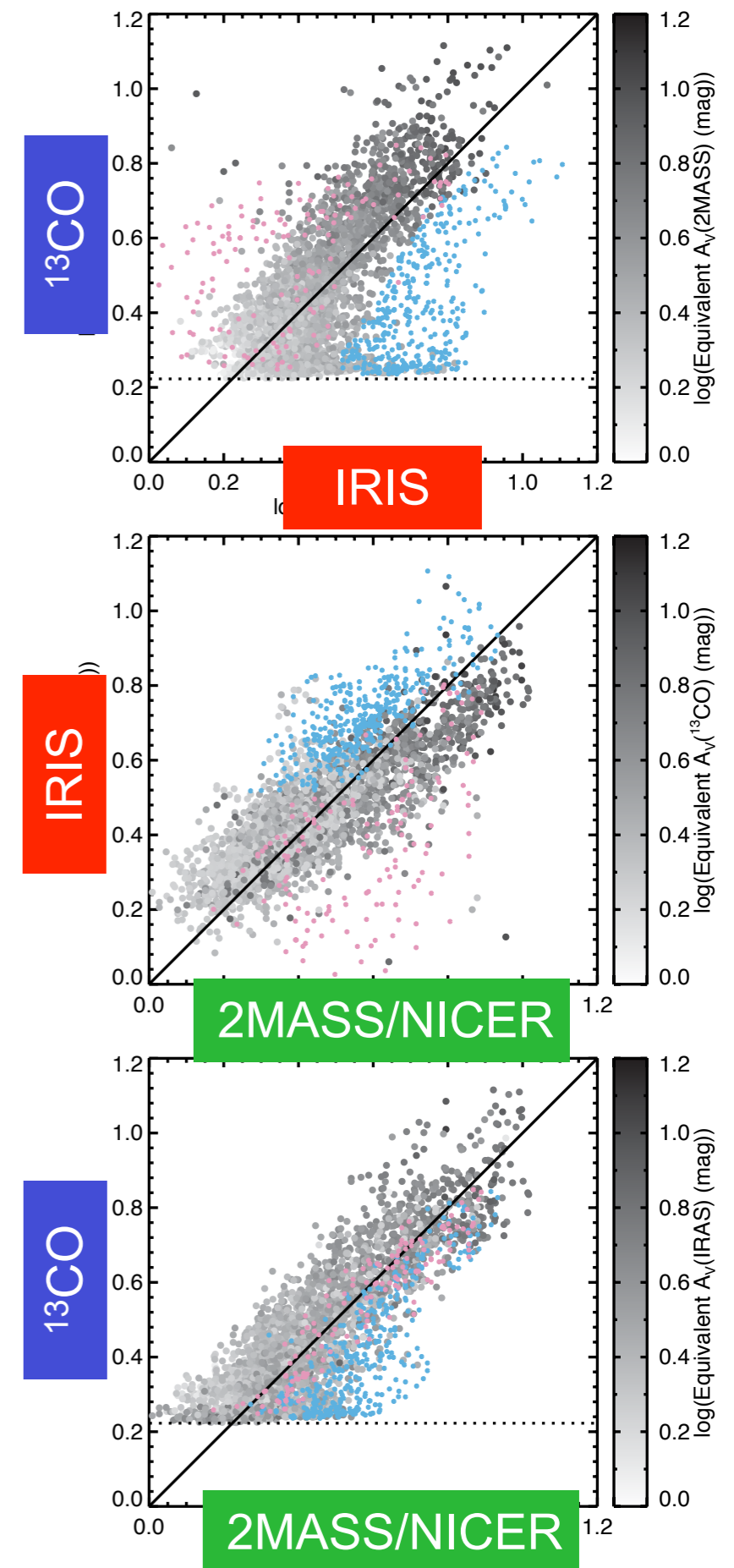
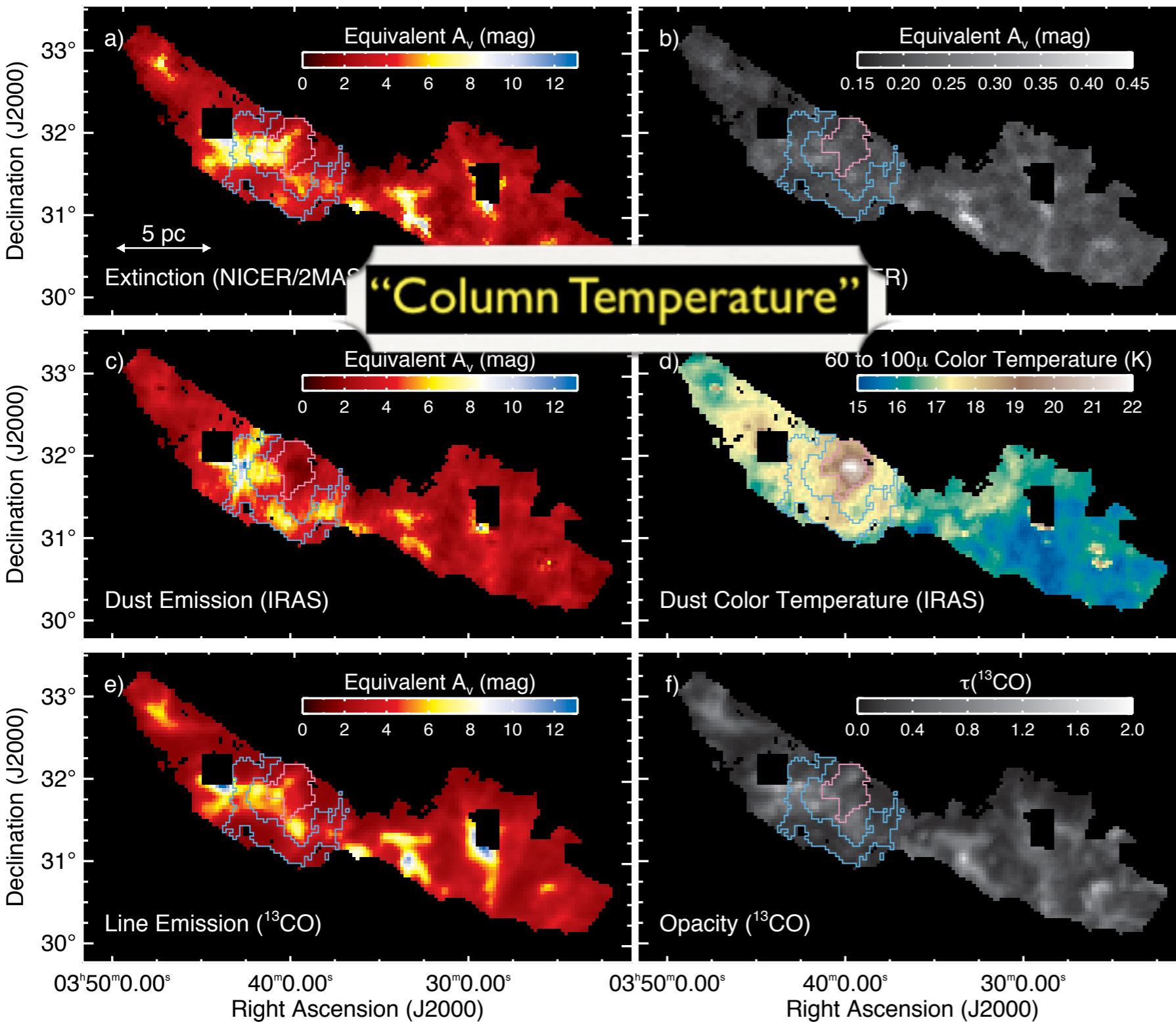
20 minutes from now...

...and more later on from...

- ★ “Column Temperature”
- ★ ^{13}CO poor tracer of column density, abundance not the problem **Caselli**
- ★ “lognormal” (*but...*)
- ★ “Cloudshine”
- ★ GNICEST (and CS!)
- ★ virial theorem over-used?
- ★ Dangers of p - p - v “observer” space
- ★ Perils of CLUMPFIND
- ★ Benefits of Dendrograms
- ★ Value of *Tasting* Dust & b-T
- ★ Spherical(!) Outflows
- ★ Cores in/out of Clusters NOT so Different
- ★ Coherent Cores are Real and they Fragment (into filaments)!? **Pineda**
- ★ SLOW motion of cores & stars w.r.t. environs
- ★ Density “thresholds” are more complicated than you think **Kauffmann**
- ★ Open Access is GOOD **Heiderman**

COMPLETE Perseus Column Density

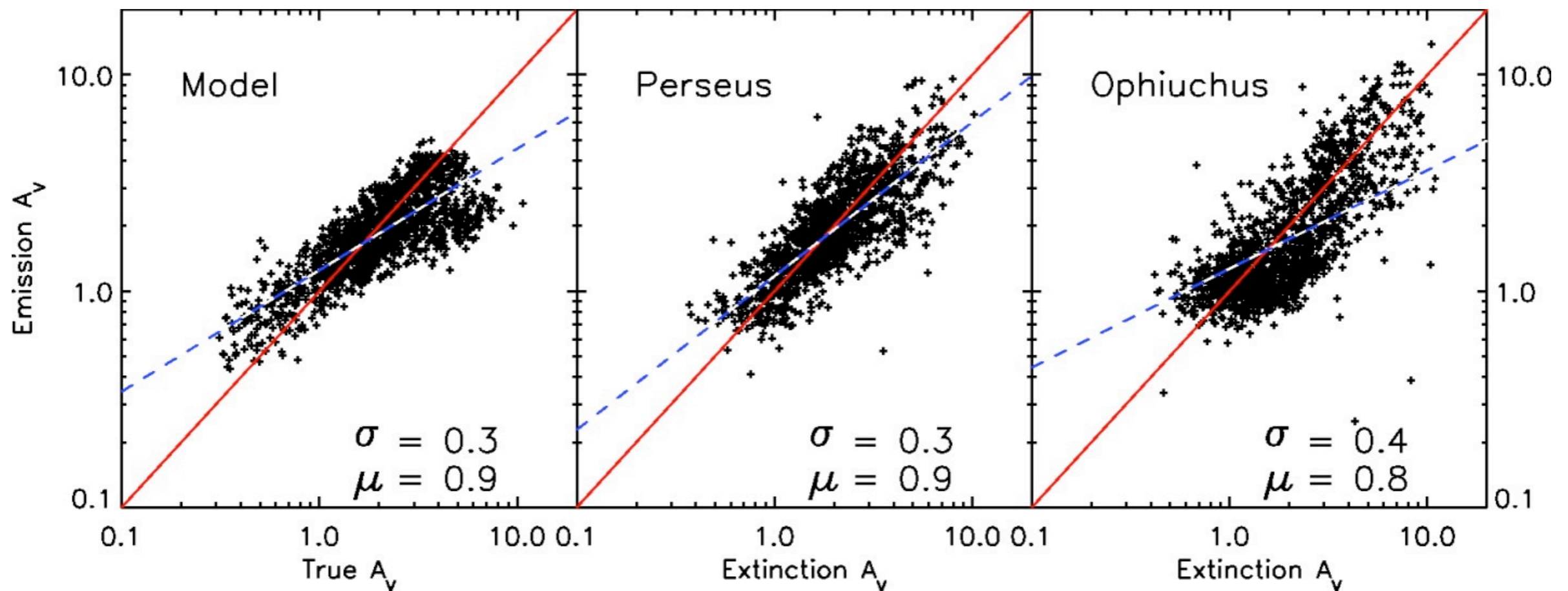
(Dust Emission, Extinction & Gas Emission)



figures: Goodman, Pineda & Schnee 2009 cf. Schnee et al. 2005, 2006, 2008; Pineda et al. 2008

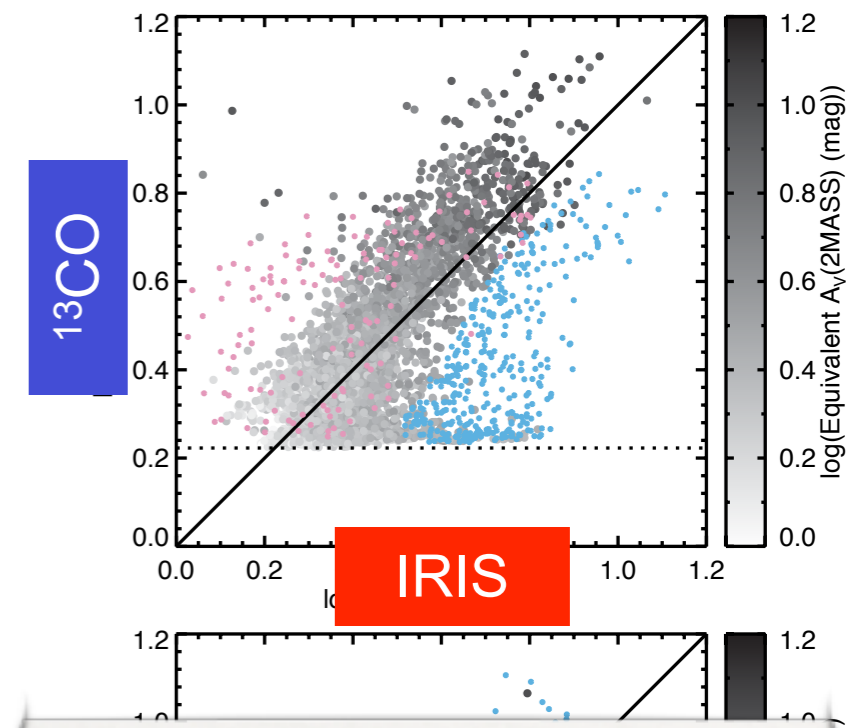
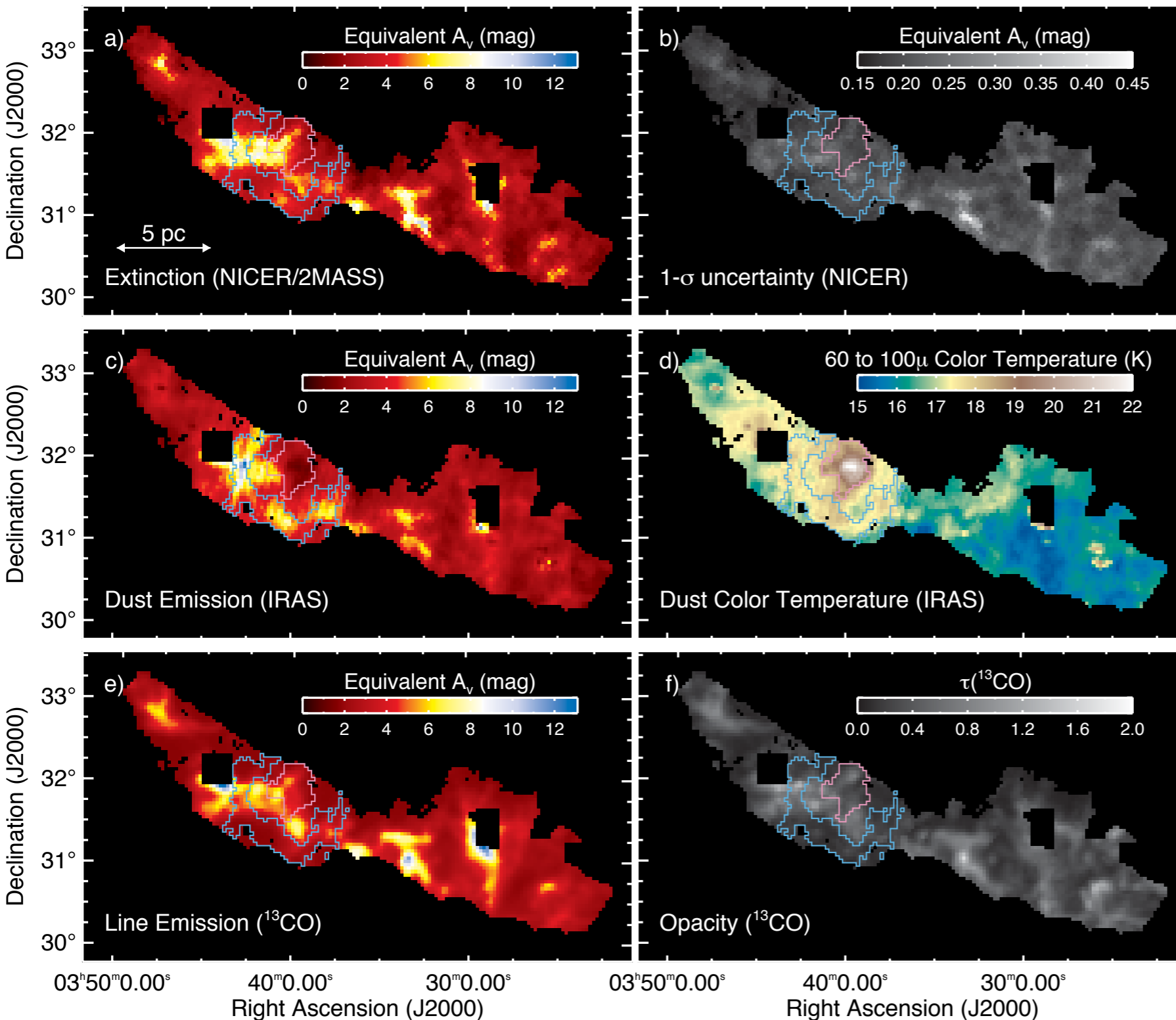
Column Temperature

And, the value of calibrating emission with extinction...

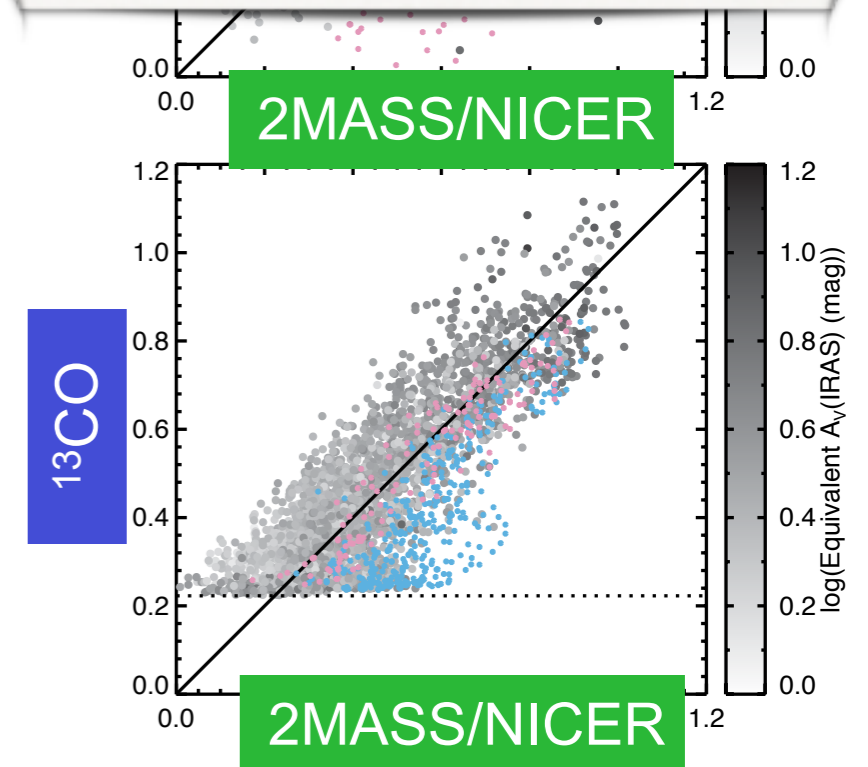


COMPLETE Perseus Column Density

(Dust Emission, Extinction & Gas Emission)

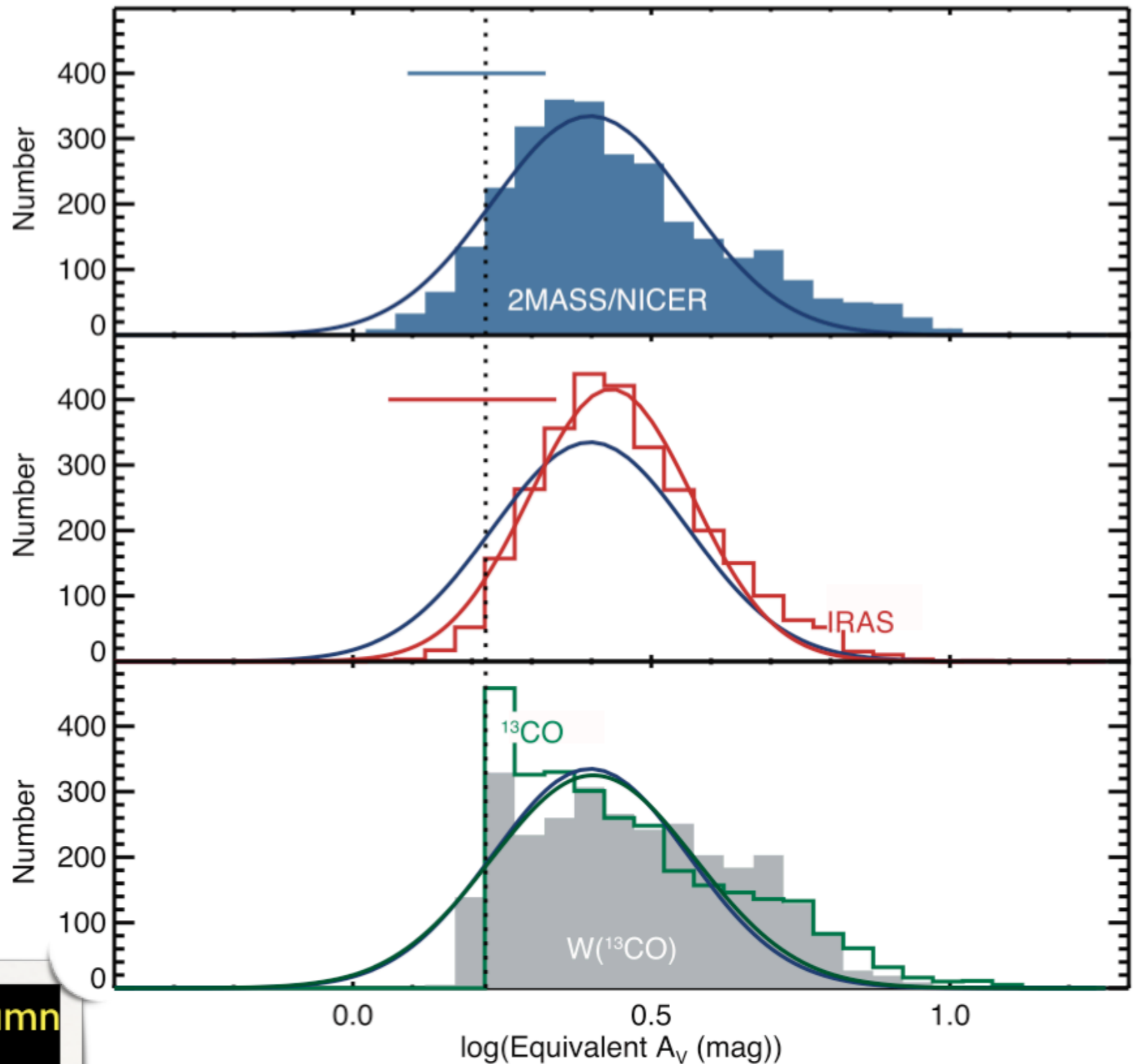


¹³CO poor tracer of column density, abundance not the problem



figures: Goodman, Pineda & Schnee 2009 cf. Schnee et al. 2005, 2006, 2008; Pineda et al. 2008

Yes, Column
Density
Distribution
is
“lognormal”
(*but...*)

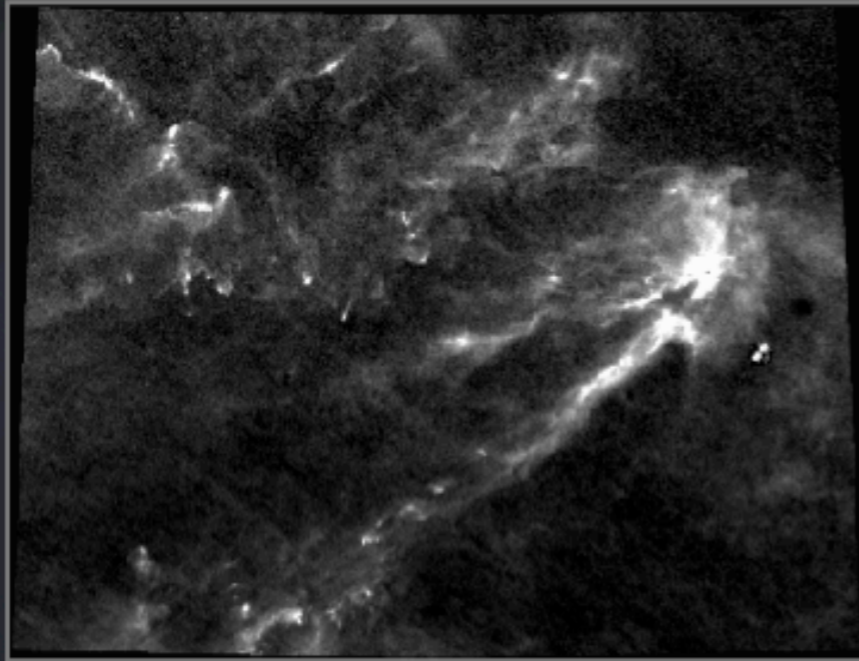


^{13}CO poor tracer of column
density, abundance not the
problem

Goodman, Pineda & Schnee 2009; Pineda et al. 2008
cf. 2MASS results of Alves, Kainulainen, Lada, Lombardi et al.

...Justin Bieber, and the IMF, can be lognormal too...

“lognormal” (but...)



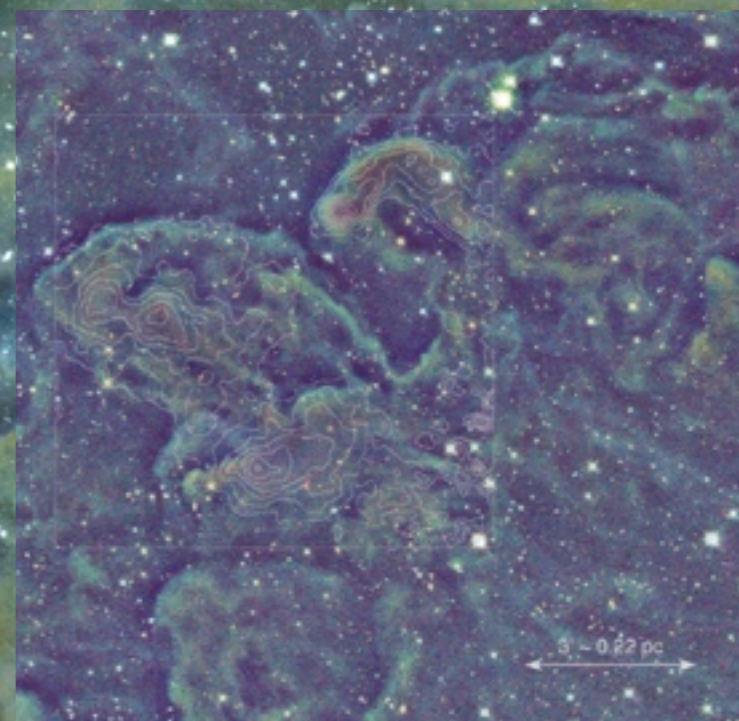
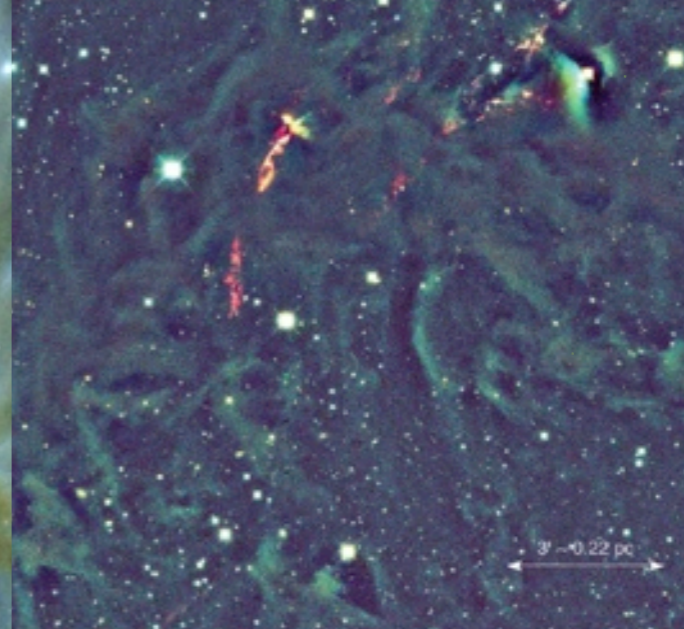
Transform!

and so is any multiplicative random process.

see Beaumont et al. 2011, and <http://www.ifa.hawaii.edu/users/beaumont/histograms/index.html>

“Cloudshine”

A happy surprise.



Background: to appear in Foster, Mandel, et al. 2011
Insets: Foster & Goodman 2006, Calar Alto JHK

Extinction Mapping

NICE, NICER, NICEST, GNICER, GNICEST (and CS!)

THE ASTROPHYSICAL JOURNAL, 674:831–845, 2008 February 20

© 2008. The American Astronomical Society. All rights reserved. Printed in U.S.A.

Ⓔ

HUNTING GALAXIES TO (AND FOR) EXTINCTION

JONATHAN B. FOSTER,¹ CARLOS G. ROMÁN-ZÚÑIGA,^{1,2} ALYSSA A. GOODMAN,¹ ELIZABETH A. LADA,³ AND JOÃO ALVES²

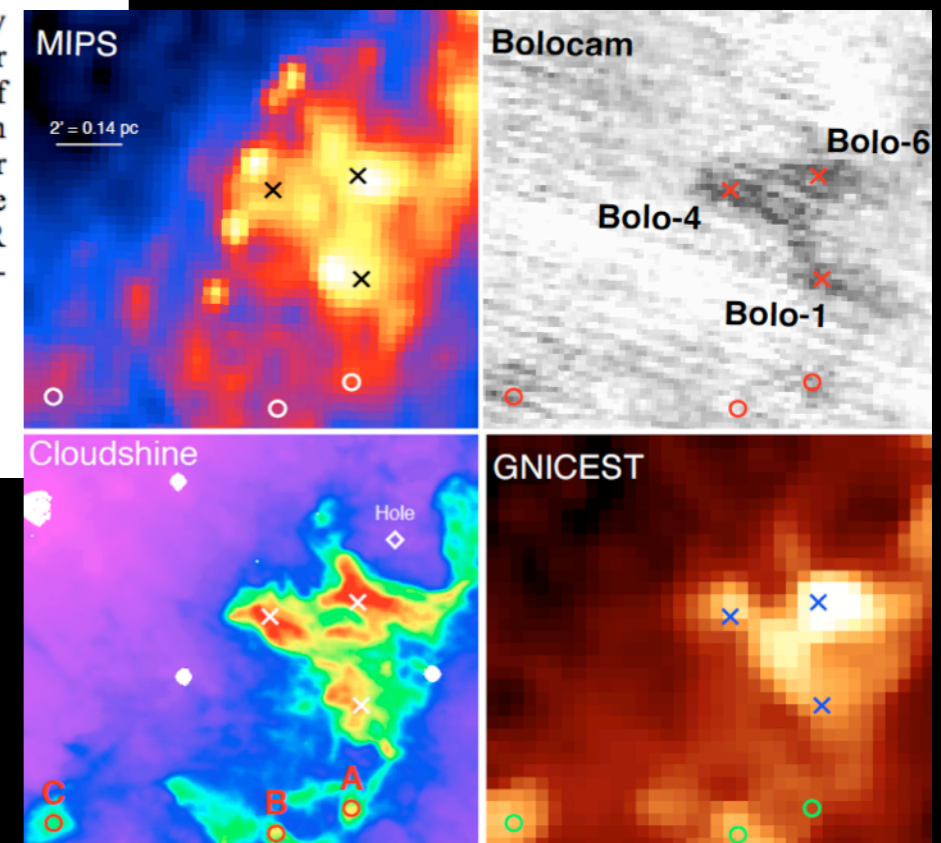
Received 2007 September 1; accepted 2007 October 28

ABSTRACT

In studies of star-forming regions, near-infrared excess (NIRX) sources—objects with intrinsic colors redder than normal stars—constitute both signal (young stars) and noise (e.g., background galaxies). We hunt down (identify) galaxies using near-infrared observations in the Perseus star-forming region by combining structural information, colors, and number density estimates. Galaxies at moderate redshifts ($z = 0.1–0.5$) have colors similar to young stellar objects (YSOs) at both near- and mid-infrared (e.g., *Spitzer*) wavelengths, which limits our ability to identify YSOs from colors alone. Structural information from high-quality near-infrared observations allows us to better separate YSOs from galaxies, rejecting two out of five of the YSO candidates identified from *Spitzer* observations of our regions and potentially extending the YSO luminosity function below K of 15 mag where galaxy contamination dominates. Once they are identified we use galaxies as valuable extra signals for making extinction maps of molecular clouds. Our new iterative procedure, the galaxies near-infrared color excess method revisited (GNICER), uses the mean colors of galaxies as a function of magnitude to include them in extinction maps in an unbiased way. GNICER increases the number of background sources used to probe the structure of a cloud, decreasing the noise and increasing the resolution of extinction maps made far from the galactic plane.

Subject headings: dust, extinction — galaxies: fundamental parameters — ISM: structure — stars: pre-main-sequence

Online material: color figures



Foster et al. 2008;

Beaumont et al. 2011 (for “CS”)

Where and when does gravity matter?

And, is the virial theorem over-used?

LETTERS

NATURE | Vol 457 | 1 January 2009

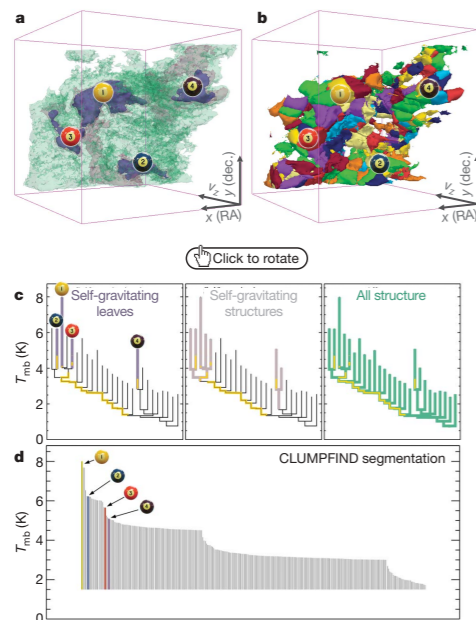


Figure 2 | Comparison of the 'dendrogram' and 'CLUMPFIND' feature-identification algorithms as applied to ^{13}CO emission from the L1448 region of Perseus. **a**, 3D visualization of the surfaces indicated by colours in the dendrogram shown in **c**. Purple illustrates the smallest scale self-gravitating structures in the region corresponding to the leaves of the dendrogram; pink shows the smallest surfaces that contain distinct self-gravitating leaves within them; and green corresponds to the surface in the data cube containing all the significant emission. Dendrogram branches corresponding to self-gravitating objects have been highlighted in yellow over the range of T_{mb} (main-beam temperature) test-level values for which the virial parameter is less than 2. The x-y locations of the four 'self-gravitating' leaves labelled with billiard balls are the same as those shown in Fig. 1. The 3D visualizations show position-position-velocity (p - p - v) space. RA, right ascension; dec., declination. For comparison with the ability of dendrograms (**c**) to track hierarchical structure, **d** shows a pseudo-dendrogram of the CLUMPFIND segmentation (**b**), with the same four labels used in Fig. 1 and in **a**. As 'clumps' are not allowed to belong to larger structures, each pseudo-branch in **d** is simply a series of lines connecting the maximum emission value in each clump to the threshold value. A very large number of clumps appears in **b** because of the sensitivity of CLUMPFIND to noise and small-scale structure in the data. In the online PDF version, the 3D cubes (**a** and **b**) can be rotated to any orientation, and surfaces can be turned on and off (interaction requires Adobe Acrobat version 7.0.8 or higher). In the printed version, the front face of each 3D cube (the 'home' view in the interactive online version) corresponds exactly to the patch of sky shown in Fig. 1, and velocity with respect to the Local Standard of Rest increases from front (-0.5 km s^{-1}) to back (8 km s^{-1}).

data, CLUMPFIND typically finds features on a limited range of scales, above but close to the physical resolution of the data, and its results can be overly dependent on input parameters. By tuning CLUMPFIND's two free parameters, the same molecular-line data set⁸ can be used to show either that the frequency distribution of clump mass is the same as the initial mass function of stars or that it follows the much shallower mass function associated with large-scale molecular clouds (Supplementary Fig. 1).

Four years before the advent of CLUMPFIND, 'structure trees'⁹ were proposed as a way to characterize clouds' hierarchical structure

using 2D maps of column density. With this early 2D work as inspiration, we have developed a structure-identification algorithm that abstracts the hierarchical structure of a 3D (p - p - v) data cube into an easily visualized representation called a 'dendrogram'¹⁰. Although well developed in other data-intensive fields^{11,12}, it is curious that the application of tree methodologies so far in astrophysics has been rare, and almost exclusively within the area of galaxy evolution, where 'merger trees' are being used with increasing frequency¹³.

Figure 3 and its legend explain the construction of dendrograms schematically. The dendrogram quantifies how and where local maxima of emission merge with each other, and its implementation is explained in Supplementary Methods. Critical to the construction of

virial theorem over-used?
Dangers of p - p - v "observer" space
Perils of CLUMPFIND
Benefits of Dendrograms

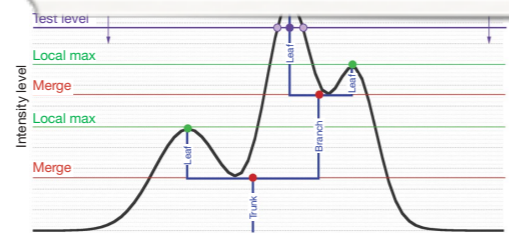


Figure 3 | Schematic illustration of the dendrogram process. Shown is the construction of a dendrogram from a hypothetical one-dimensional emission profile (black). The dendrogram (blue) can be constructed by 'dropping' a test constant emission level (purple) from above in tiny steps (exaggerated in size here, light lines) until all the local maxima and mergers are found, and connected as shown. The intersection of a test level with the emission is a set of points (for example the light purple dots) in one dimension, a planar curve in two dimensions, and an isosurface in three dimensions. The dendrogram of 3D data shown in Fig. 2c is the direct analogue of the tree shown here, only constructed from 'isosurface' rather than 'point' intersections. It has been sorted and flattened for representation on a flat page, as fully representing dendrograms for 3D data cubes would require four dimensions.

IS the virial theorem over-used?

Possible to Determine Nature of Clumps

Possible to Determine Nature of Clumps

Classic Param

Simple Structure (Simple Sphere)






Complex Structure (Highly Filamentary)

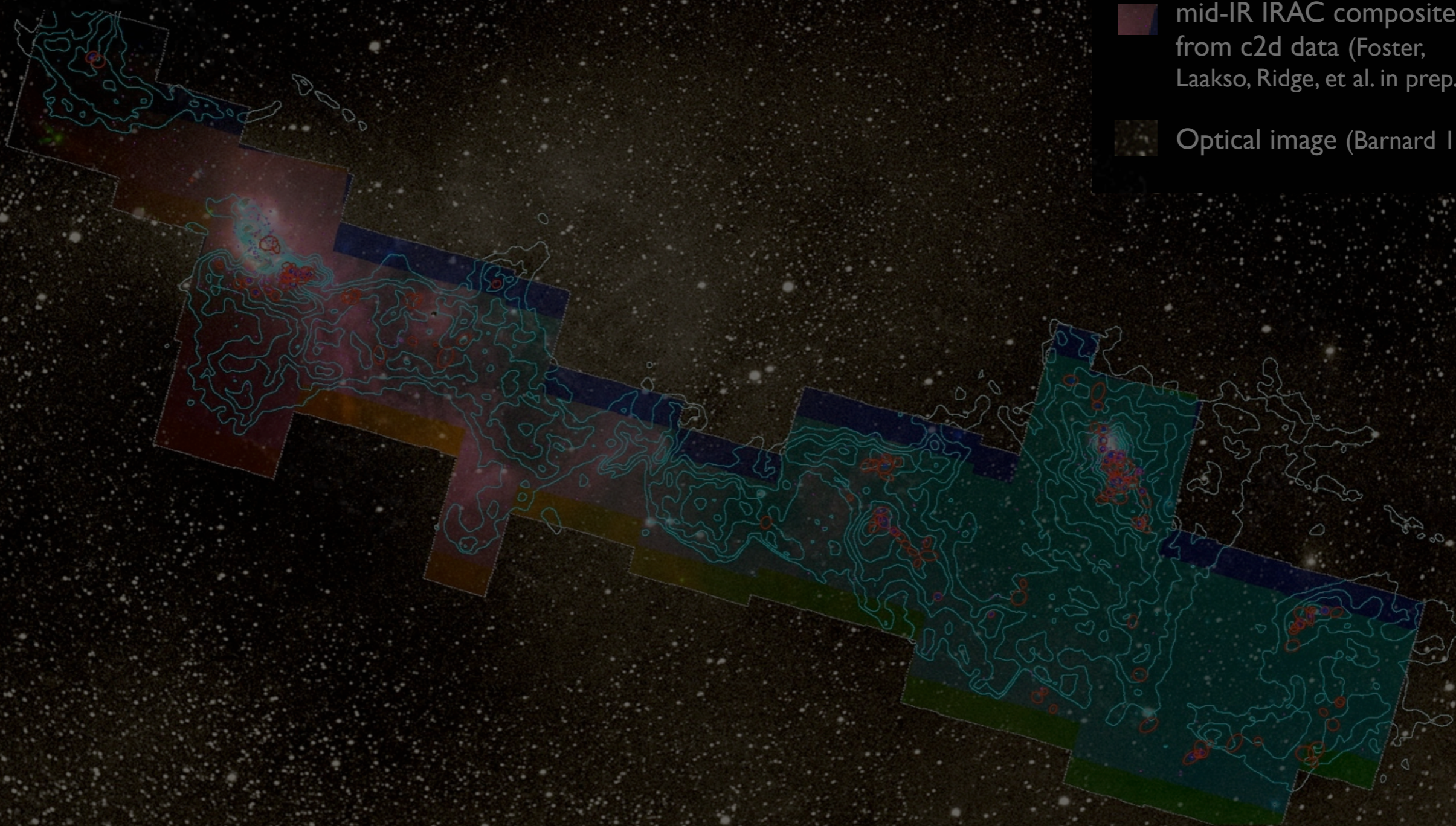
Cloud Structure

Figure 7. Schematic diagram indicating how the consideration of more complex physics is possibly required to reliably assess whether structures in molecular clouds are bound or not. The abscissa represents the level of complexity in the cloud, from a relatively simple sphere to a highly filamentary cloud. The ordinate represents the physical process considered in the analysis. The circle and cross represent cases we have considered in this work.

COMPLETE Perseus

Image size: 1305 x 733
VL: 63 WW: 127

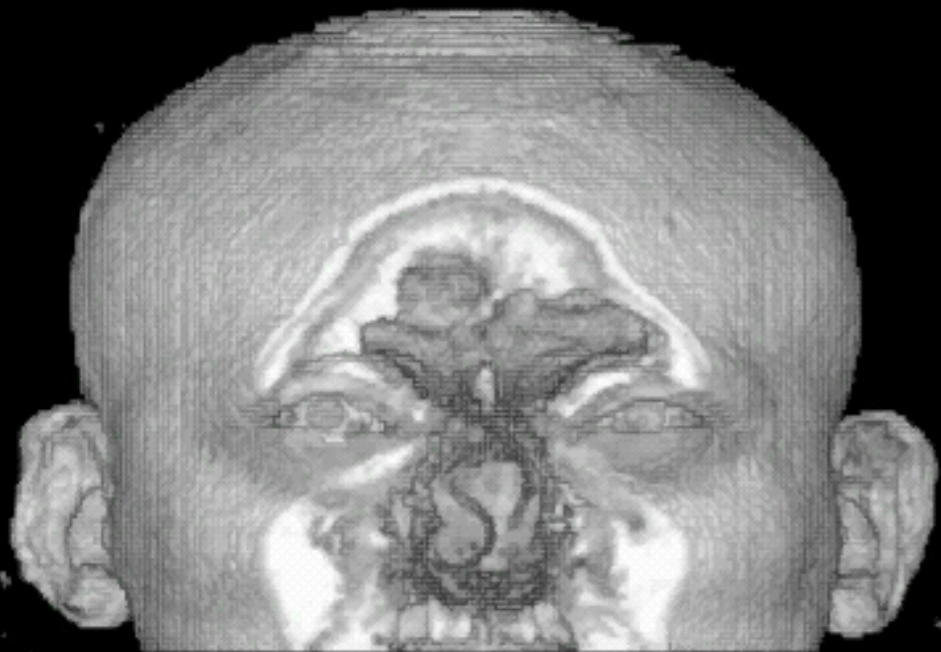
-  mm peak (Enoch et al. 2006)
-  sub-mm peak (Hatchell et al. 2005, Kirk et al. 2006)
-  ^{13}CO (Ridge et al. 2006)
-  mid-IR IRAC composite from c2d data (Foster, Laakso, Ridge, et al. in prep.)
-  Optical image (Barnard 1927)



m: 17249
Zoom: 227% Angle: 0

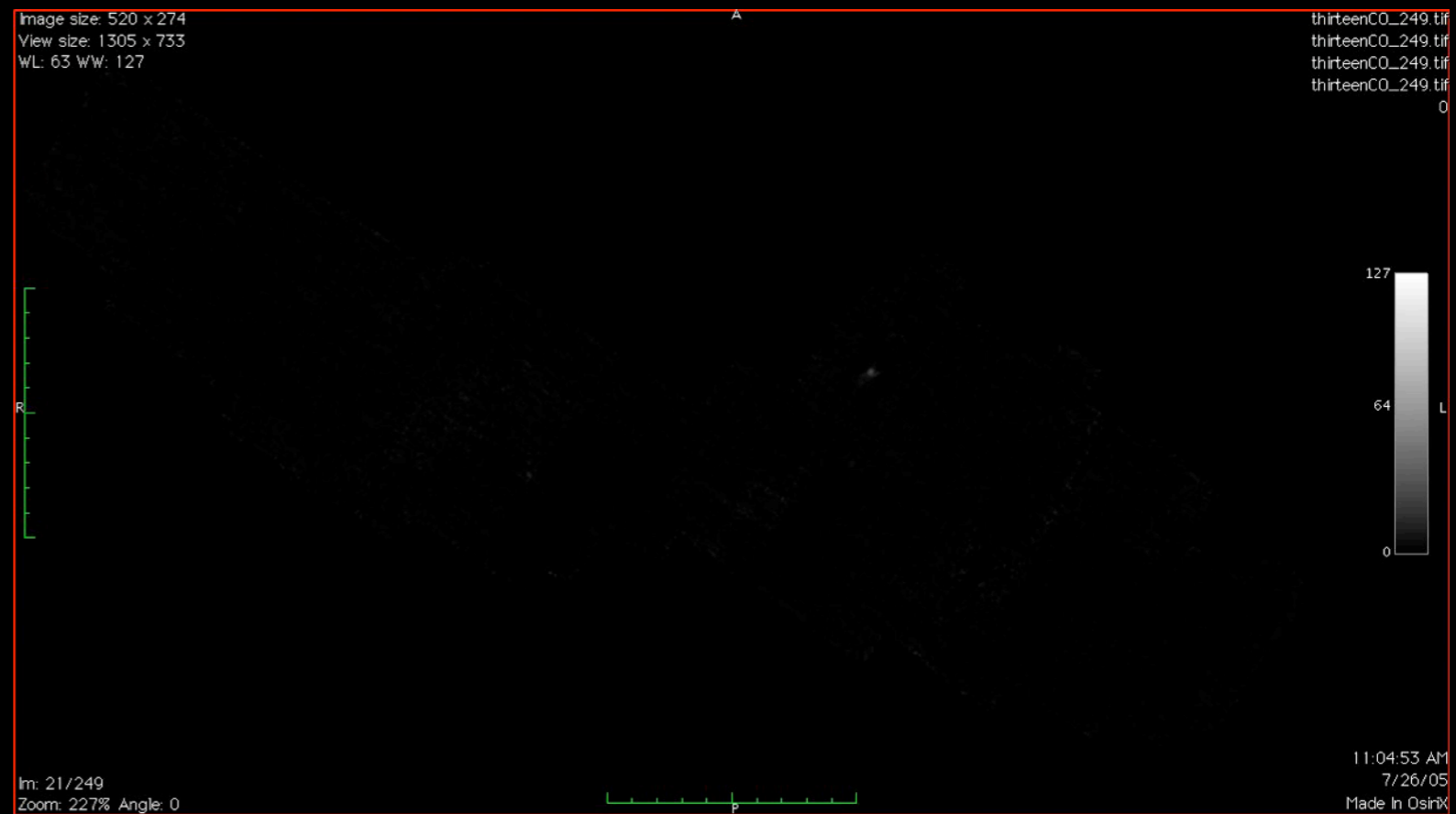
Value of High-Dimensional Visualization and “Taste-Testing”... *p-p-v* space, and more...

“KEITH”

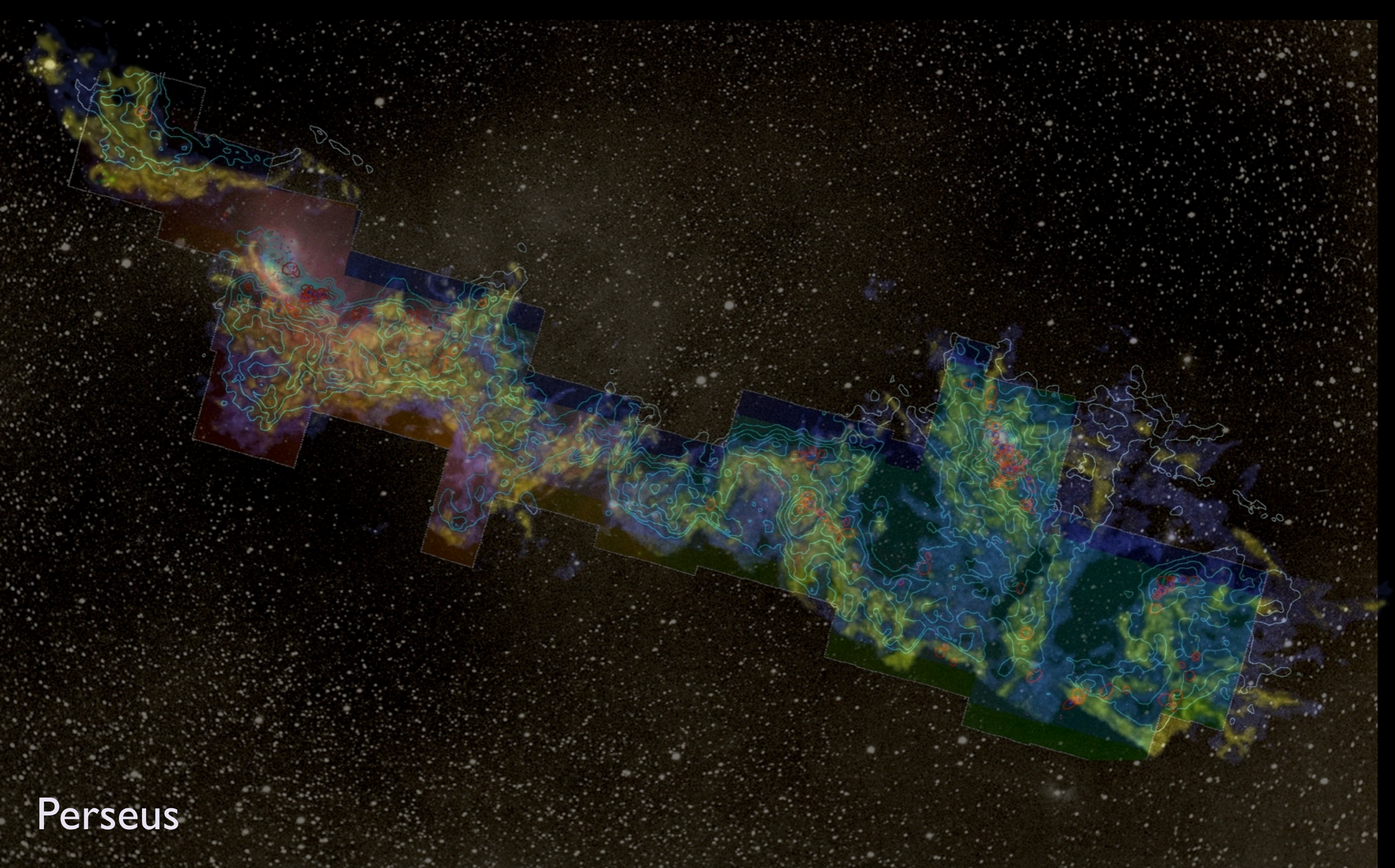


“z” is depth into head

“PERSEUS”



“z” is line-of-sight velocity



Perseus

3D Viz made with VolView

Where and when does gravity matter?

And, is the virial theorem over-used?

LETTERS

NATURE | Vol 457 | 1 January 2009

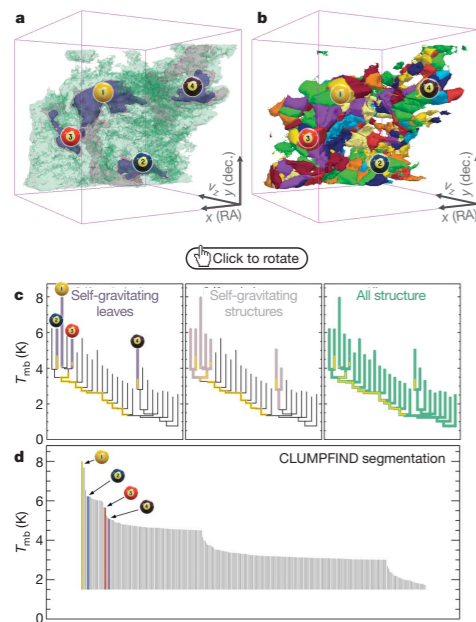


Figure 2 | Comparison of the 'dendrogram' and 'CLUMPFIND' feature-identification algorithms as applied to ^{13}CO emission from the L1448 region of Perseus. **a**, 3D visualization of the surfaces indicated by colours in the dendrogram shown in **c**. Purple illustrates the smallest scale self-gravitating structures in the region corresponding to the leaves of the dendrogram; pink shows the smallest surfaces that contain distinct self-gravitating leaves within them; and green corresponds to the surface in the data cube containing all the significant emission. Dendrogram branches corresponding to self-gravitating objects have been highlighted in yellow over the range of T_{mb} (main-beam temperature) test-level values for which the virial parameter is less than 2. The x-y locations of the four 'self-gravitating' leaves labelled with billiard balls are the same as those shown in Fig. 1. The 3D visualizations show position-position-velocity ($p-p-v$) space. RA, right ascension; dec., declination. For comparison with the ability of dendrograms (**c**) to track hierarchical structure, **d** shows a pseudo-dendrogram of the CLUMPFIND segmentation (**b**), with the same four labels used in Fig. 1 and in **a**. As 'clumps' are not allowed to belong to larger structures, each pseudo-branch in **d** is simply a series of lines connecting the maximum emission value in each clump to the threshold value. A very large number of clumps appears in **b** because of the sensitivity of CLUMPFIND to noise and small-scale structure in the data. In the online PDF version, the 3D cubes (**a** and **b**) can be rotated to any orientation, and surfaces can be turned on and off (interaction requires Adobe Acrobat version 7.0.8 or higher). In the printed version, the front face of each 3D cube (the 'home' view in the interactive online version) corresponds exactly to the patch of sky shown in Fig. 1, and velocity with respect to the Local Standard of Rest increases from front (-0.5 km s^{-1}) to back (8 km s^{-1}).

data, CLUMPFIND typically finds features on a limited range of scales, above but close to the physical resolution of the data, and its results can be overly dependent on input parameters. By tuning CLUMPFIND's two free parameters, the same molecular-line data set⁸ can be used to show either that the frequency distribution of clump mass is the same as the initial mass function of stars or that it follows the much shallower mass function associated with large-scale molecular clouds (Supplementary Fig. 1).

Four years before the advent of CLUMPFIND, 'structure trees'⁹ were proposed as a way to characterize clouds' hierarchical structure

using 2D maps of column density. With this early 2D work as inspiration, we have developed a structure-identification algorithm that abstracts the hierarchical structure of a 3D ($p-p-v$) data cube into an easily visualized representation called a 'dendrogram'¹⁰. Although well developed in other data-intensive fields^{11,12}, it is curious that the application of tree methodologies so far in astrophysics has been rare, and almost exclusively within the area of galaxy evolution, where 'merger trees' are being used with increasing frequency¹³.

Figure 3 and its legend explain the construction of dendrograms schematically. The dendrogram quantifies how and where local maxima of emission merge with each other, and its implementation is explained in Supplementary Methods. Critical to the construction of

virial theorem over-used?
Dangers of $p-p-v$ "observer" space
Perils of CLUMPFIND
Benefits of Dendrograms

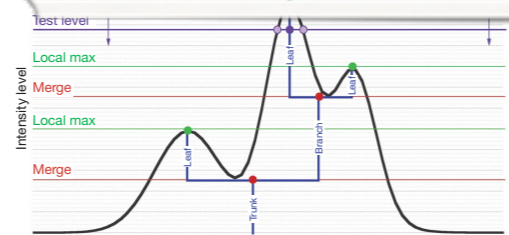


Figure 3 | Schematic illustration of the dendrogram process. Shown is the construction of a dendrogram from a hypothetical one-dimensional emission profile (black). The dendrogram (blue) can be constructed by 'dropping' a test constant emission level (purple) from above in tiny steps (exaggerated in size here, light lines) until all the local maxima and mergers are found, and connected as shown. The intersection of a test level with the emission is a set of points (for example the light purple dots) in one dimension, a planar curve in two dimensions, and an isosurface in three dimensions. The dendrogram of 3D data shown in Fig. 2c is the direct analogue of the tree shown here, only constructed from 'isosurface' rather than 'point' intersections. It has been sorted and flattened for representation in this figure. 'Representing dendrograms for 3D data cubes would be...

64

©2009 Macmillan Publisher



IS the virial theorem over-used?

iter +
ms
All Physics

Possible to Determine Nature of Clumps

Possible to
rmine Nature of Clumps

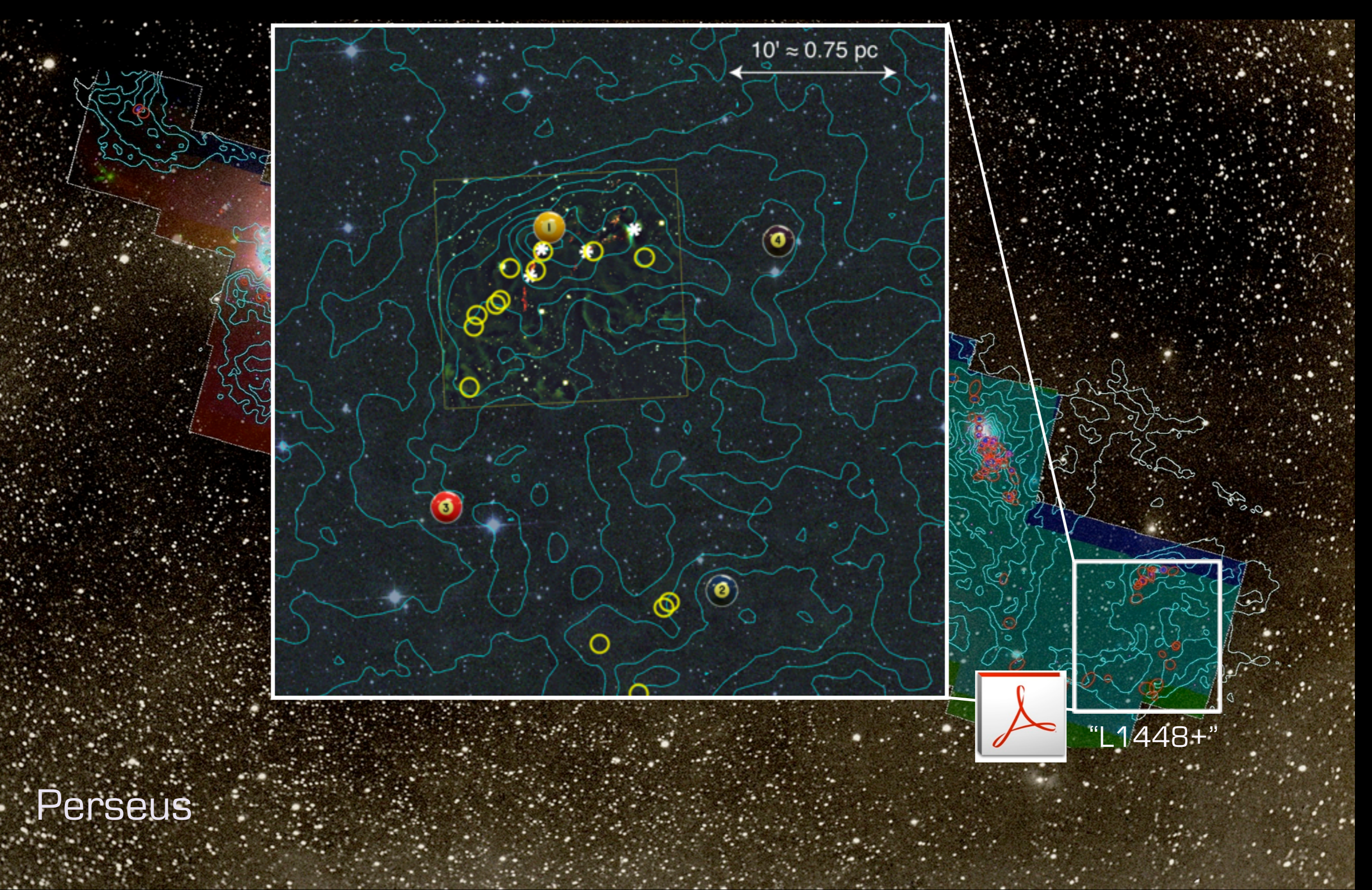
Classi
Param

Simple Structure
(Simple Sphere)

Complex Structure
(Highly Filamentary)

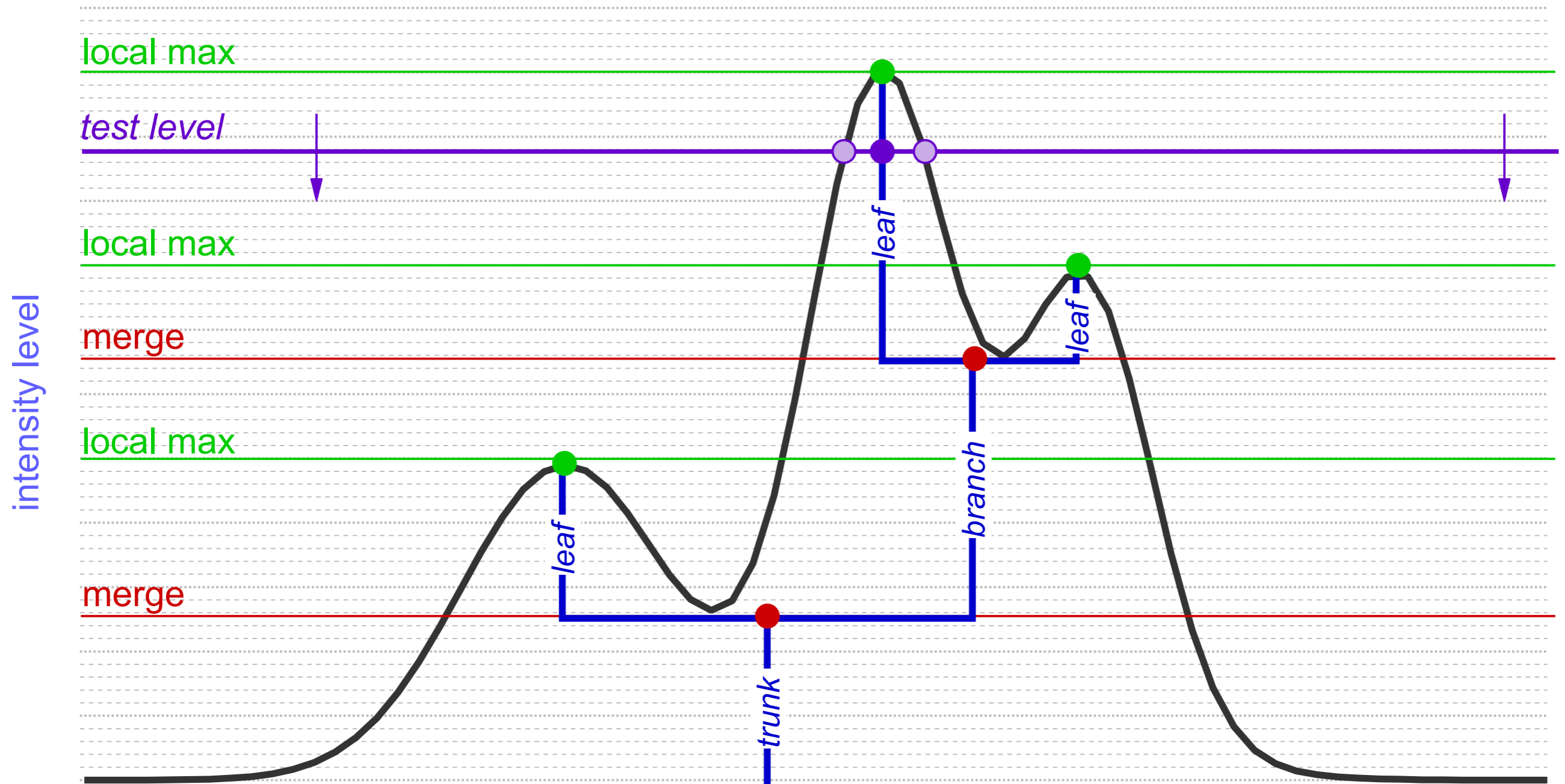
Cloud Structure

Figure 7. Schematic diagram indicating how the consideration of more complex physics is possibly required to reliably assess whether structures in molecular clouds are bound or not. The abscissa represents the level of complexity in the cloud, from a relatively simple sphere to a highly filamentary cloud. The ordinate represents the physical process considered in the analysis. The circle and cross represent cases we have considered in this work.



Perseus

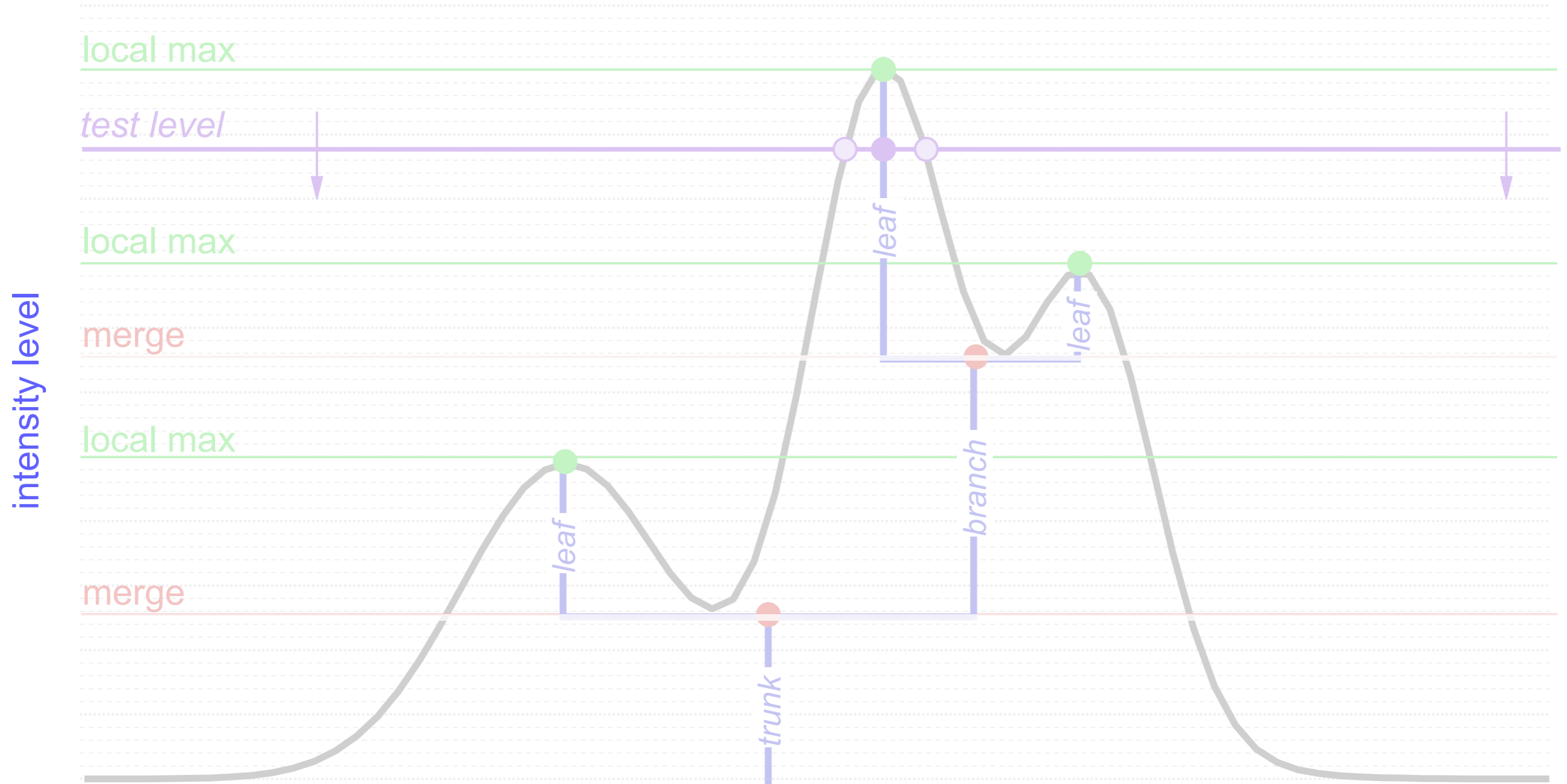
Dendrograms



Hierarchical "Segmentation"

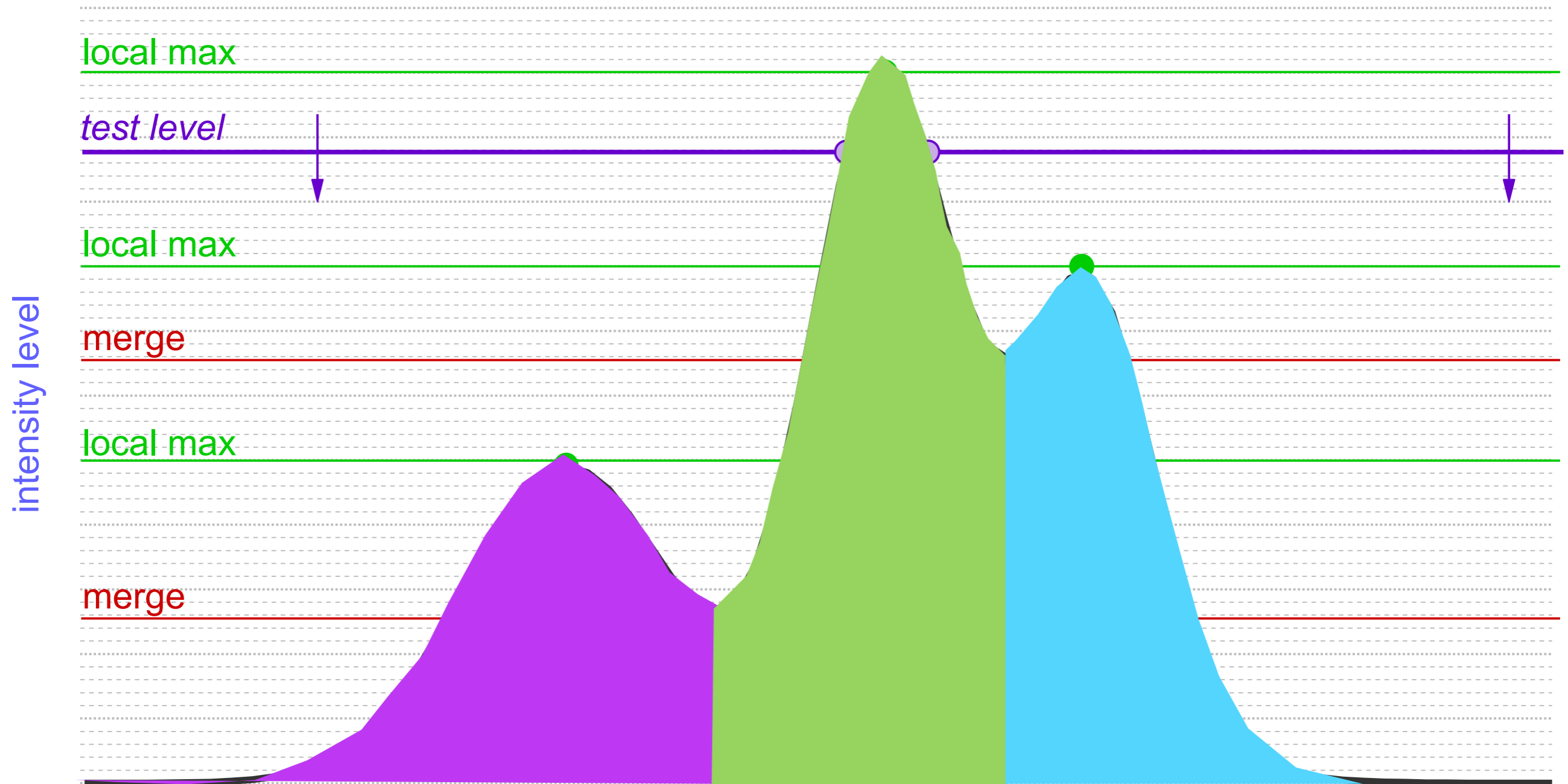
Rosolowsky, Pineda, Kauffmann & Goodman 2008

Dendrograms



1-D: points; 2-D closed curves (contours); 3-D surfaces enclosing volumes
see 2D demo at <http://am.iic.harvard.edu/index.cgi/DendroStar/applet>

What would *CLUMPFIND* do?



No hierarchy is allowed, all clumps go to the baseline.
(Williams, De Geus & Blitz 1994)

CLUMPFIND

“Crowded” 3D data
(very dangerous)

“Sparse” 2D data
(OK)

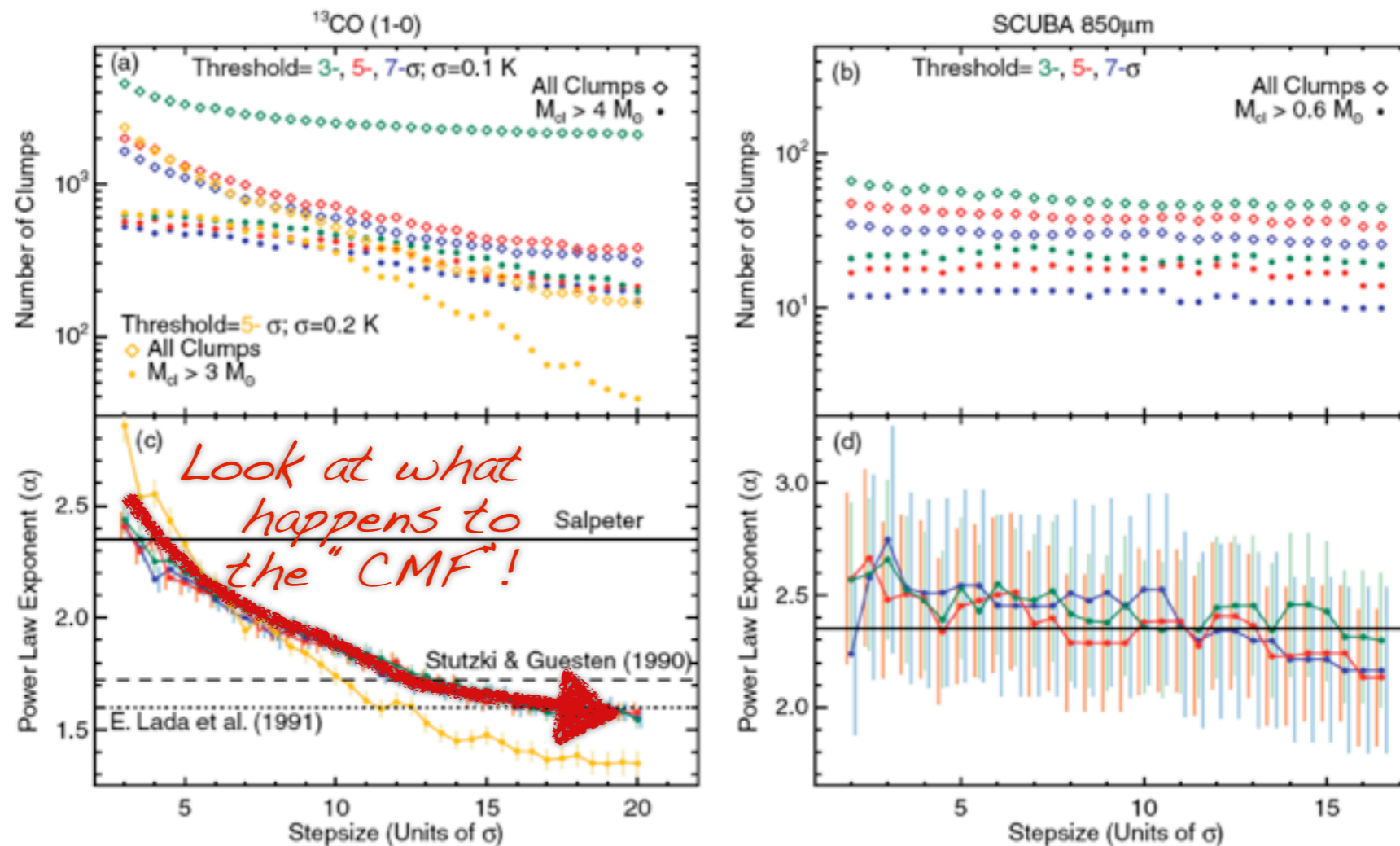
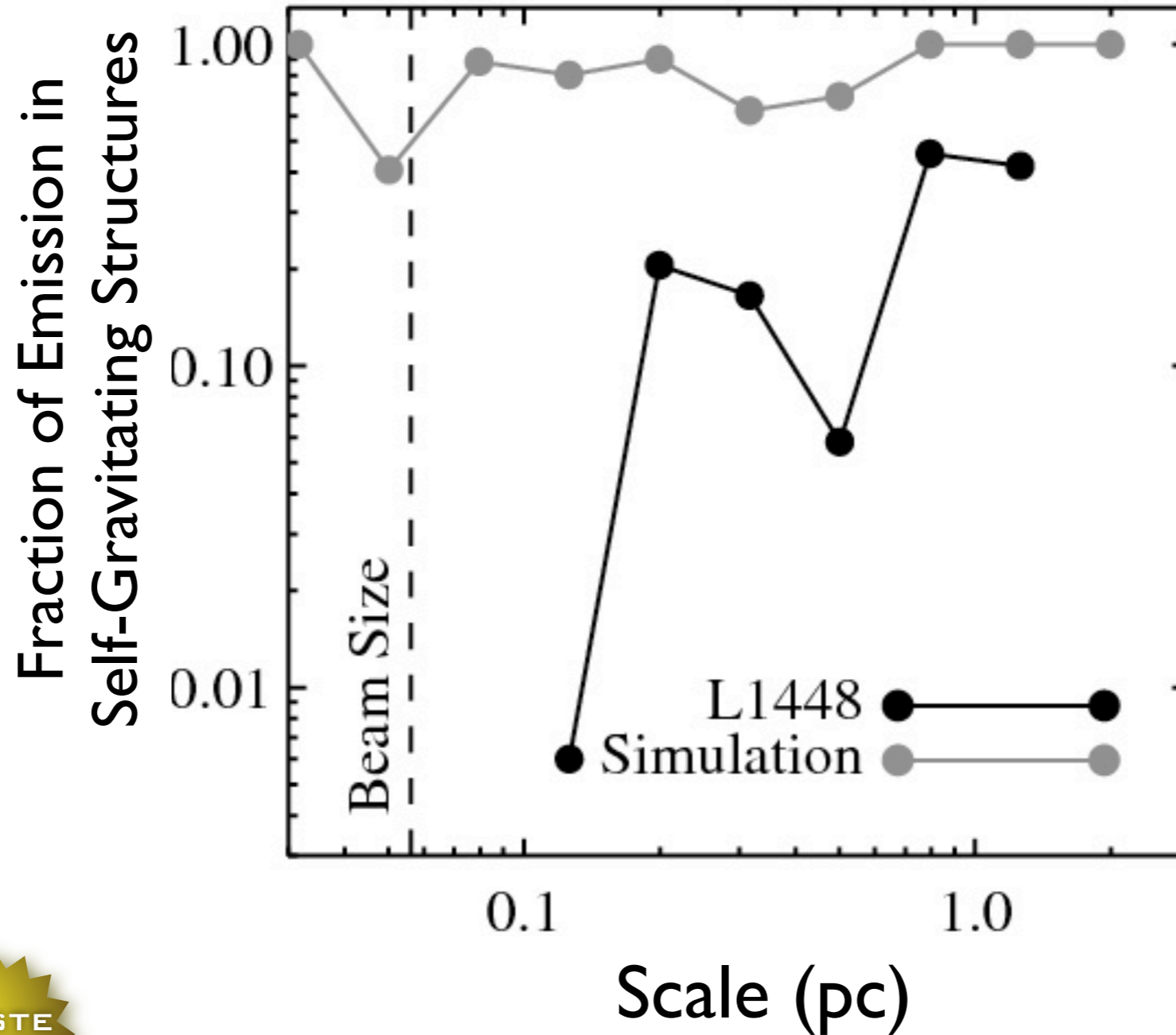


Figure 2. Summary of all Clumpfind runs as a function of stepsize. Color represent different thresholds: blue, red, and green for 3σ , 5σ , and 7σ , respectively; we also show in orange results with a threshold of 5σ for ^{13}CO data with added noise. Left and right columns show results for ^{13}CO and SCUBA data, respectively. Panels (a) and (b) show the number of clumps under a given category per model. Total number of clumps found, and total number of clumps with mass larger than the completeness limit are shown in open diamonds and filled circles, respectively. Panels (c) and (d) show the exponent of the fitted mass spectrum of clumps above the completeness limit, $dN/dM \propto M^{-\alpha}$, with error bars estimated from Equation (6). Horizontal black lines show some fiducial exponents for comparison. Average noise in ^{13}CO , ^{13}CO with added noise, and SCUBA data is 0.1 K , 0.2 K , and 0.06 Jy beam^{-1} , respectively. Completeness limit is estimated to be $4 M_{\odot}$, $3 M_{\odot}$, and $0.6 M_{\odot}$ for ^{13}CO , ^{13}CO with added noise, and SCUBA data. Panel (c) also shows that for different noise level in the data, if a threshold of $\sim 2\text{ K}$ (20σ and 10σ for original and noise-added data, respectively) is used, then the fitted power-law exponents are closer to previous works.

from “**The Perils of CLUMPFIND**” by Pineda et al. 2009

Taste-Testing “Gravity”



Gravity-free HD Simulations from Padoan et al. 2006;
 L1448 analysis from Rosolowsky et al. 2008, Goodman et al. 2009
 both lines derived from ^{13}CO “observations”

LETTERS NATURE | Vol 457 | January 2009

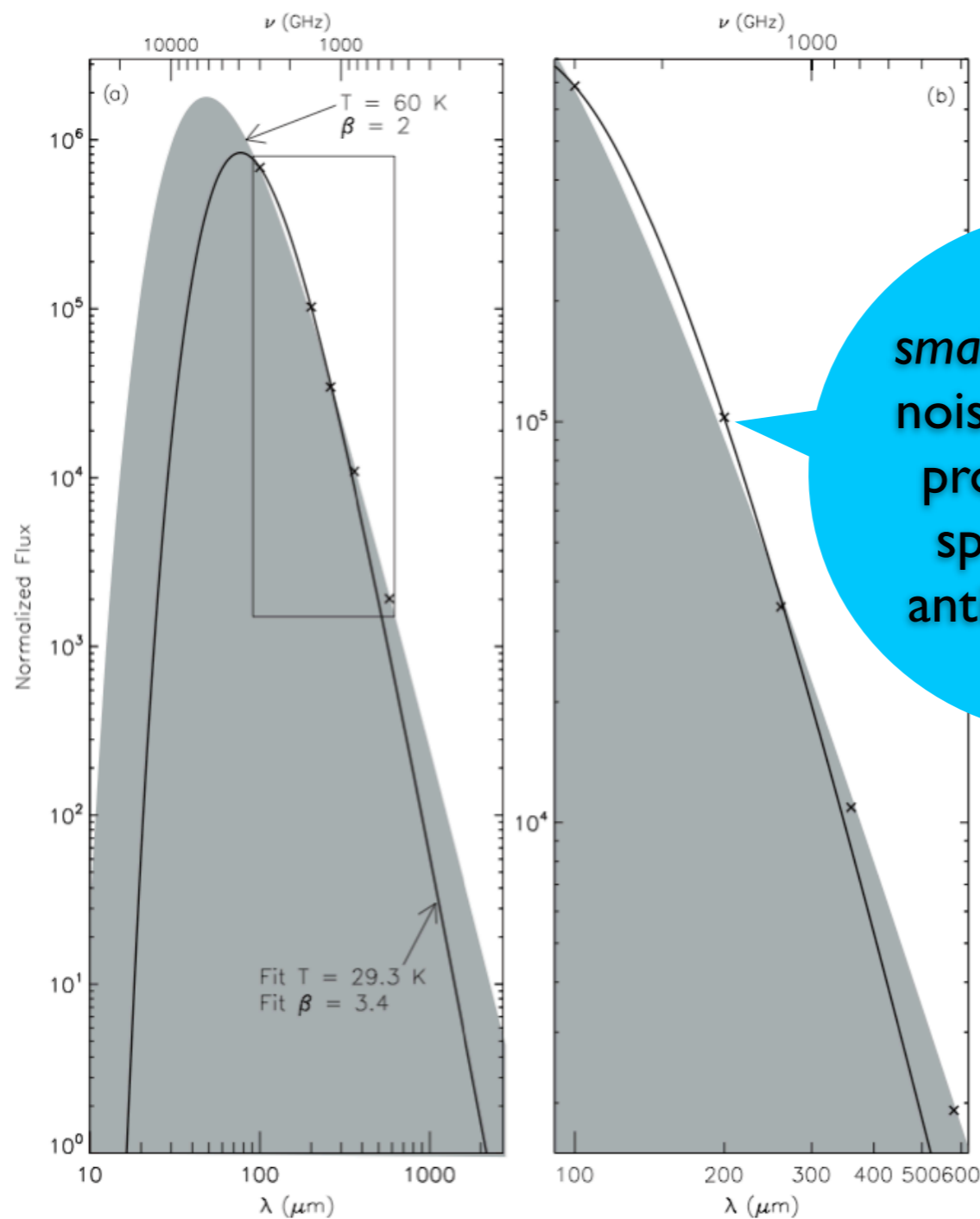
Figure 2 Comparison of the ‘dendrogram’ and ‘CLUMPFIND’ feature-identification algorithms as applied to ^{13}CO emission from the L1448 region of Perseus. **a**, 3D visualization of the surface indicated by colours in the dendrogram shown in **c**. Purple illustrates the smallest scale self-gravitating structures in the region corresponding to the leaves of the dendrogram; pink shows the smallest surfaces that contain distinct self-gravitating layers within them; and green corresponds to the surface in the data cube containing all the significant emission. Dendrogram branches corresponding to self-gravitating objects have been highlighted in yellow over the range of T_{mb} (main-beam temperature) test-level values for which the virial parameter is less than 2. The x - y locations of the four ‘self-gravitating’ leaves labelled with billiard balls are the same as those shown in Fig. 1. The 3D visualizations show position-position-velocity (p - p - v) space. **b**, **c**, right ascension, declination. For comparison with the ability of dendrograms (**c**) to track hierarchical structure, **d** shows a pseudo-dendrogram of the CLUMPFIND segmentation (**b**), with the same four labels used in Fig. 1 and in **a**. As ‘clumps’ are not allowed to belong to larger structures, each pseudo-branch in **d** is simply a series of lines connecting the maximum emission value in each clump to the threshold value. A very large number of clumps appears in **d** because of the sensitivity of CLUMPFIND to noise and small-scale structure in the data. In the online PDF version, the 3D cubes (**a** and **b**) can be rotated to any orientation, and surfaces can be turned on and off (interaction requires Adobe Acrobat version 7.0.8 or higher). In the printed version, the front face of each 3D cube (the ‘home’ view in the interactive online version) corresponds exactly to the patch of sky shown in Fig. 1, and velocity with respect to the Local Standard of Rest increases from front (-33.3 km s^{-1}) to back (0 km s^{-1}).

Figure 3 Schematic illustration of the dendrogram process. Shown is the construction of a dendrogram from a hypothetical one-dimensional emission profile (black). The dendrogram (blue) can be constructed by ‘dropping’ a test constant emission level (purple) from above in tiny steps (exaggerated in size here; light lines) until the local maxima and mergers are found, and connected as shown. The intersection of a test level with the emission is a set of points (for example the light purple dots) in one dimension, a planar curve in two dimensions, and an isosurface in three dimensions. The dendrogram of 3D data shown in Fig. 2c is the direct analogue of the tree shown here, only constructed from ‘isosurfaces’ rather than ‘points’ intersections. It has been sorted and flattened for representation on a flat page, as fully representing dendrograms for 3D data cubes would require four dimensions.

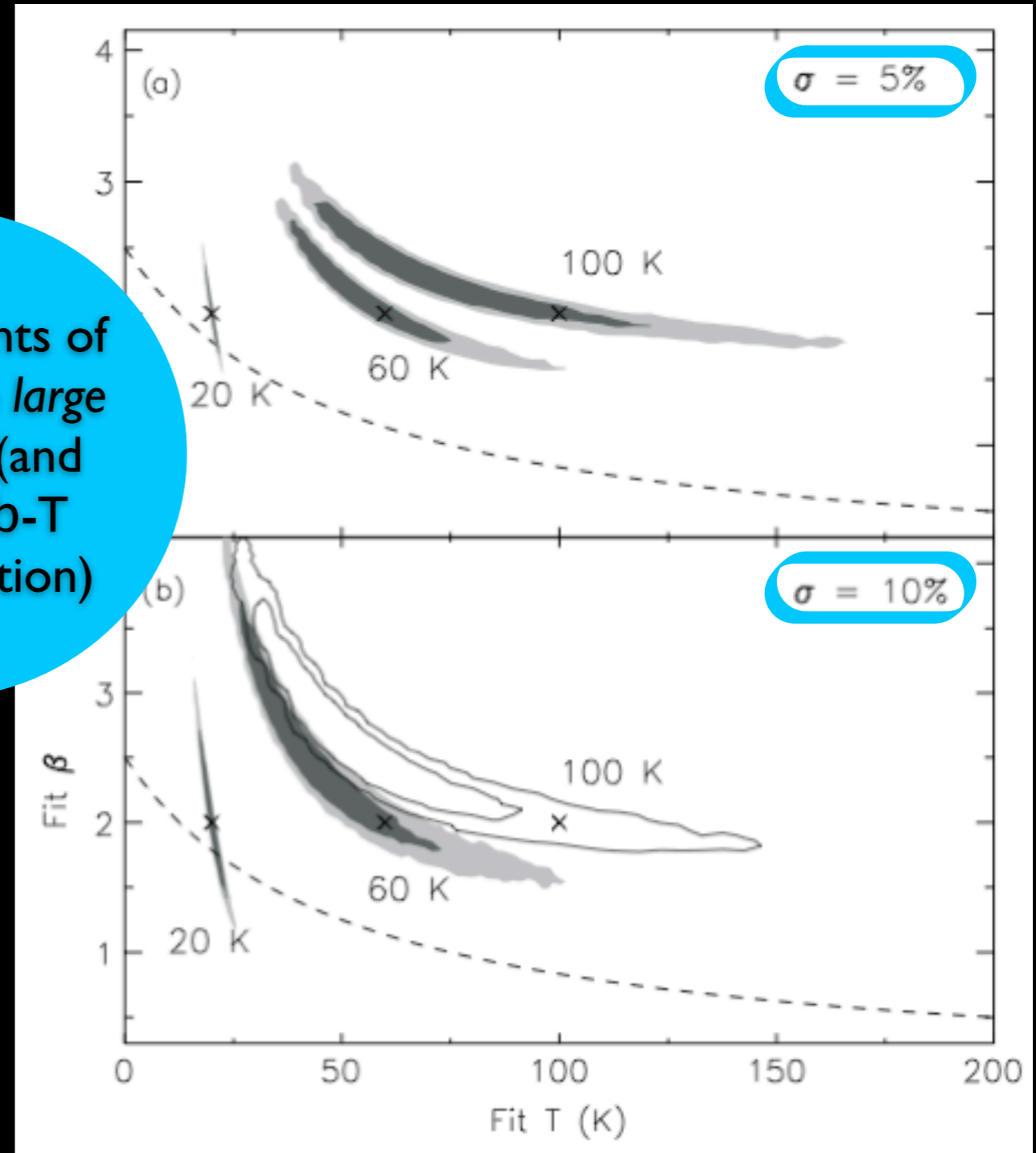
44 © 2009 Macmillan Publishers Limited. All rights reserved

Taste-Testing...

Value of *Tasting* Dust & b-T



small amounts of noise cause *large* problems (and spurious b-T anticorrelation)



Shetty et al. 2009a, b; and see improved SED analysis method upcoming in Kelly et al. 2011 (in prep.)

Outflows

Bipolar & Spherical(!)

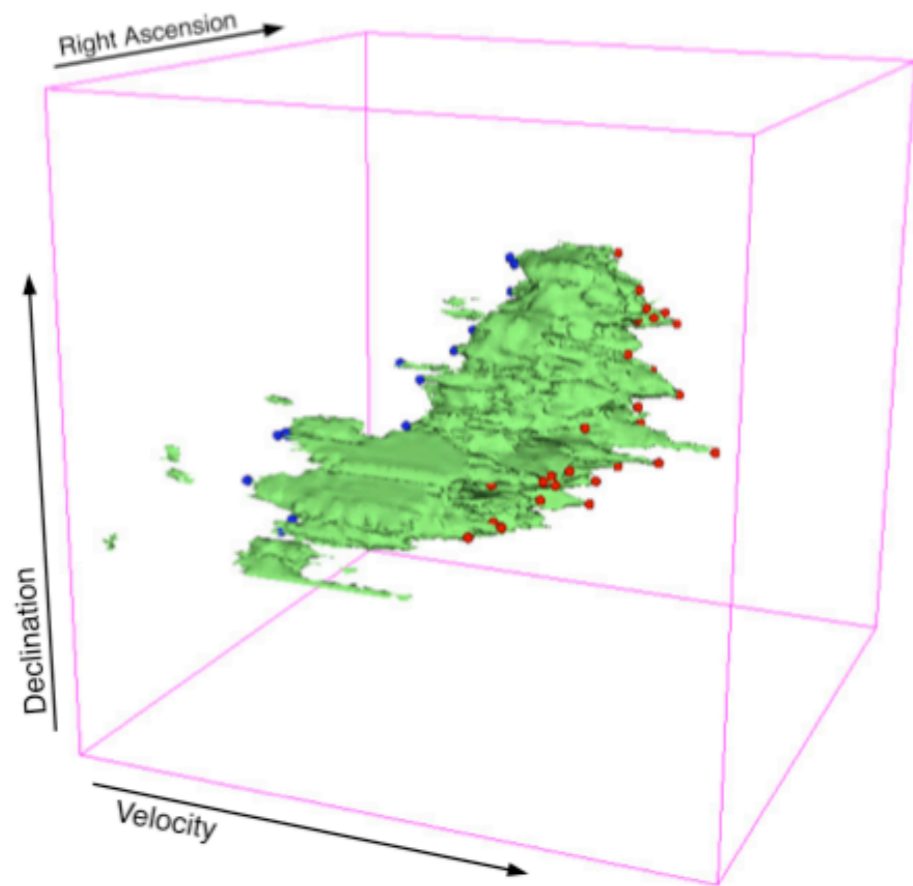
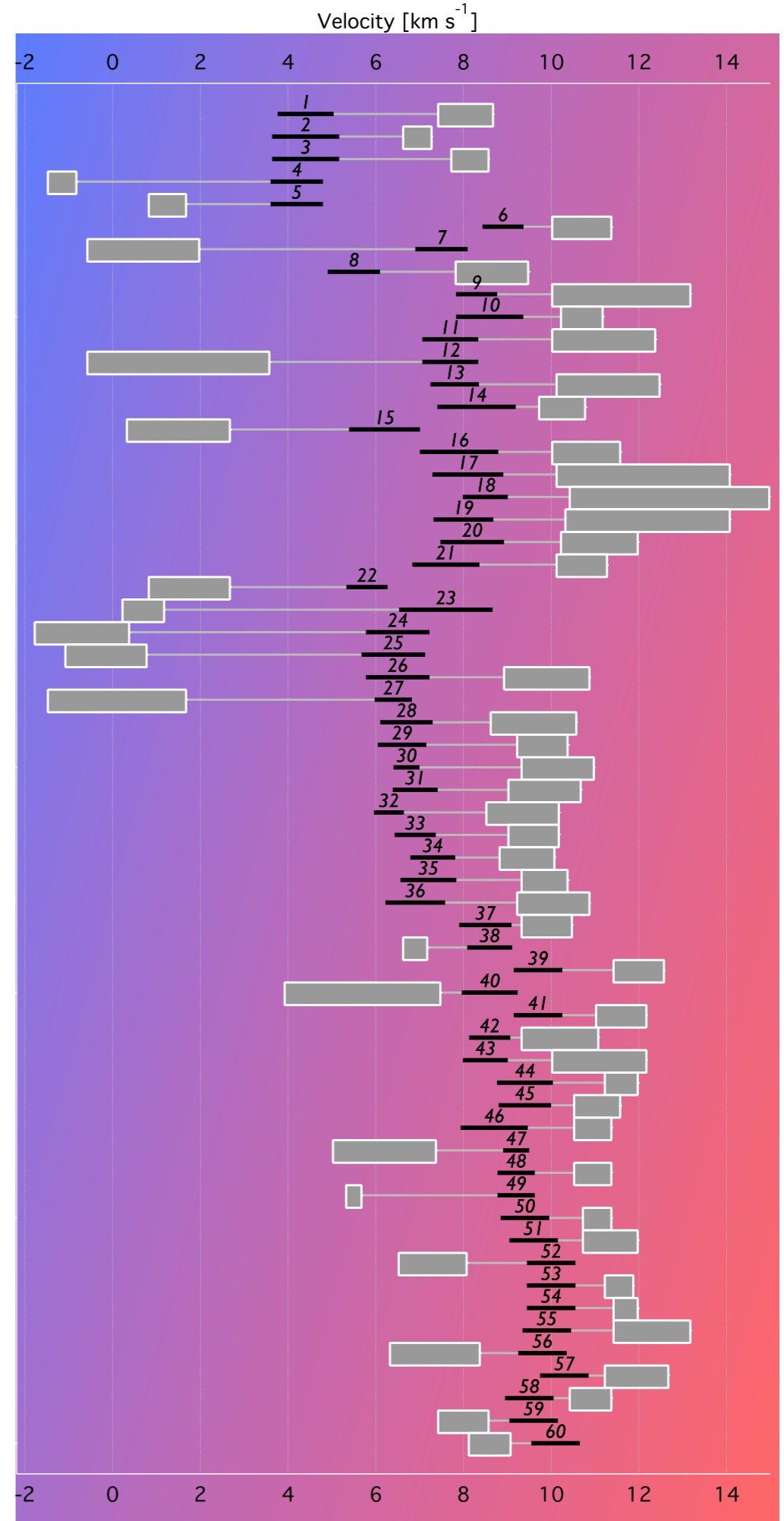


Figure 2. Three-dimensional rendering of the molecular gas in B5 (i.e., Area VI in Figure 1), using 3D Slicer. The gray (green) isosurface model shows the ^{12}CO emission in position–position–velocity space. The small circles show the locations of identified high-velocity points (with the color in the online version representing whether the point is blue- or red-shifted).

Arce et al. 2010, 2011



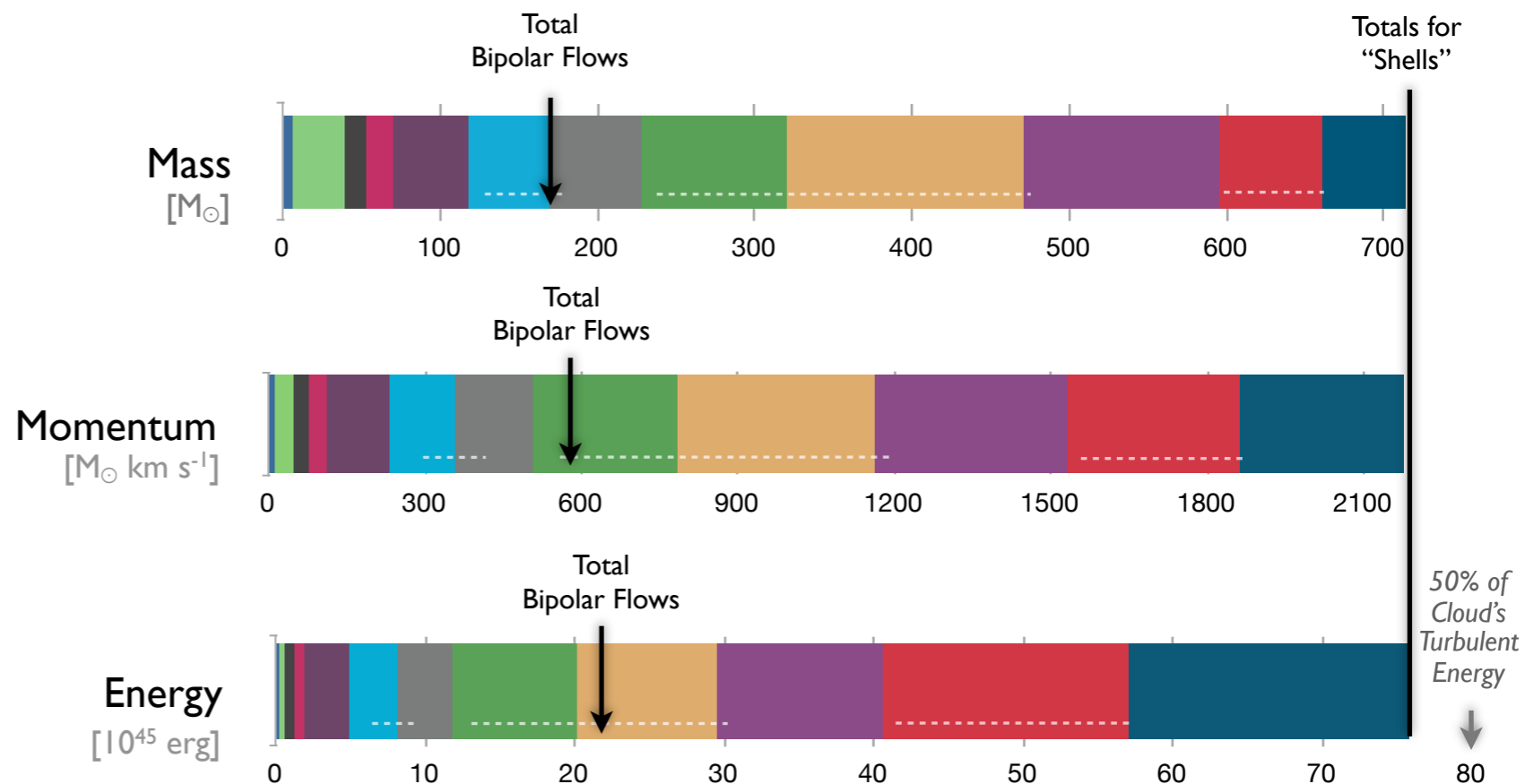
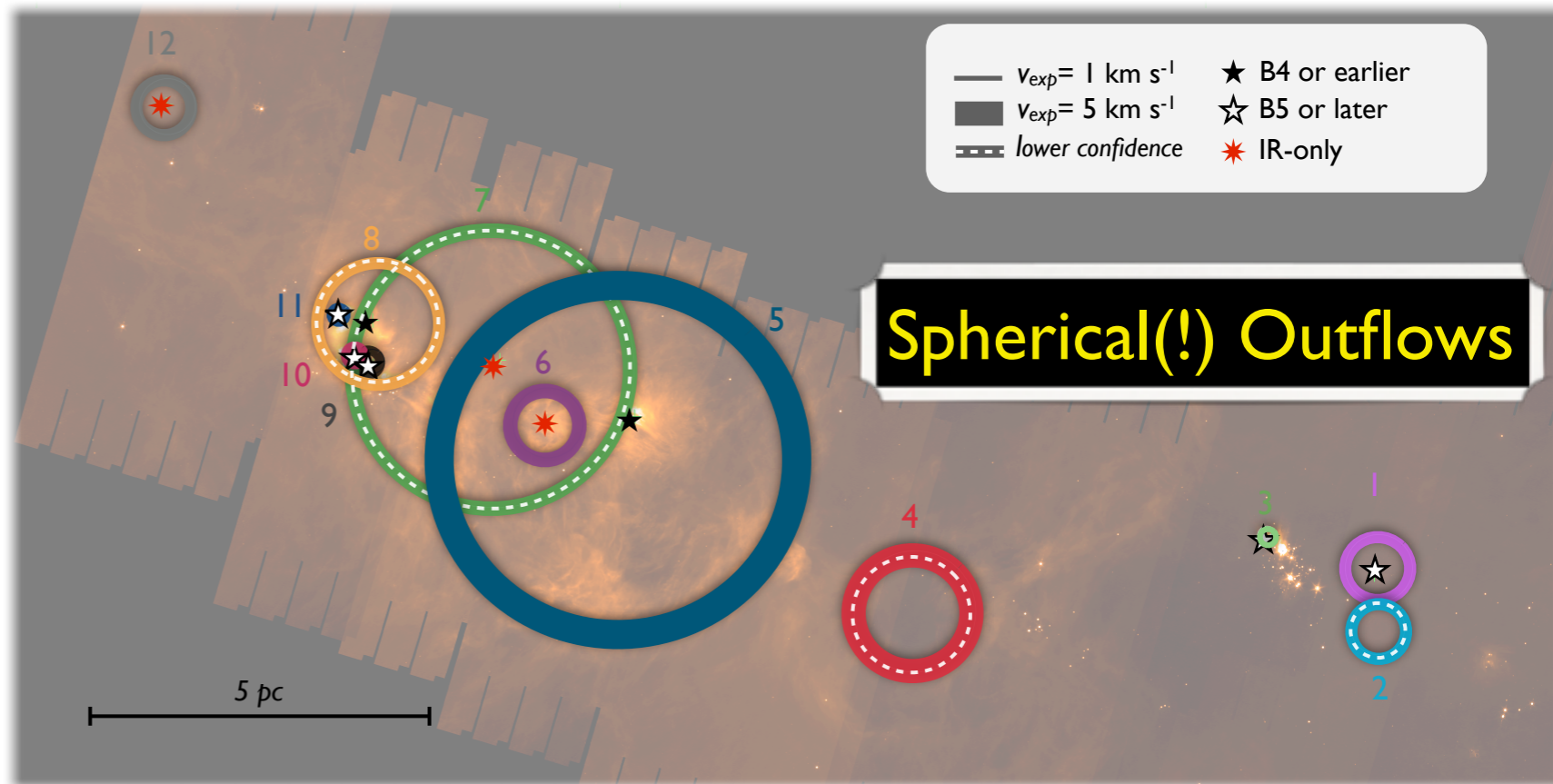
Outflows

Bipolar & Spherical(!)

News Flash

Spherical shells from young-ish stars may stir molecular clouds (much) MORE than bipolar flows, and B-stars may matter much.

Arce et al. 2011
(in press, on astro-ph)



Cores in and out of clusters

NOT so different! (Once cores are “ungrouped”...)

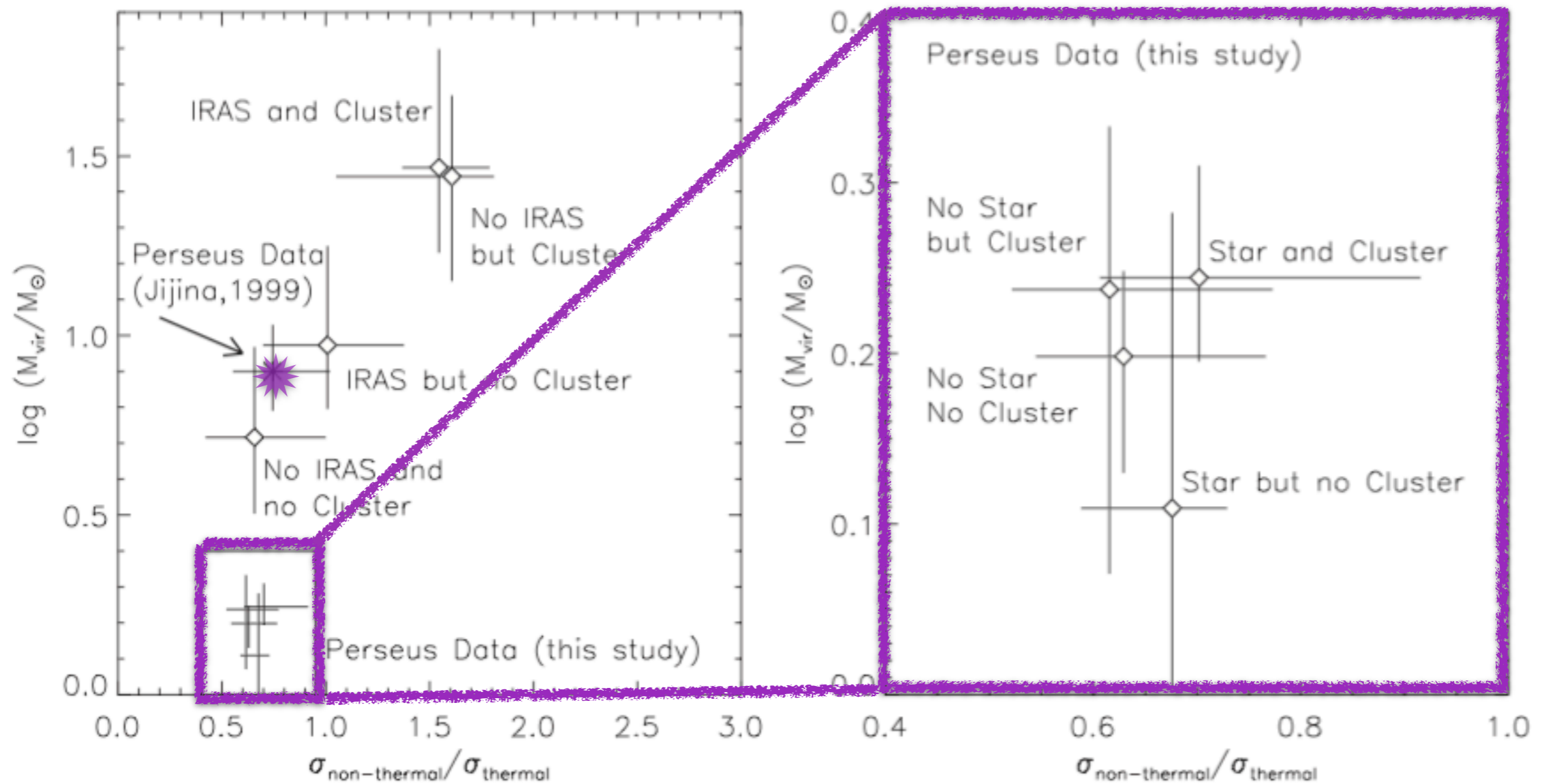


Figure 12. Median and quartile $\log(M_{\text{vir}}/M_{\odot})$ vs. $\sigma_{\text{nonthermal}}/\sigma_{\text{thermal}}$ for the four different subsamples of objects as in Figure 4 from Jijina et al. (1999). On the left, the Jijina et al. (1999) results (IRAS point sources were used as a proxy for protostellar), which span a much larger range in both axes and exhibit more separation between classifications than our Perseus data. Cores in Perseus from the Jijina et al. (1999) database are typically more massive. We zoom into our data on the right, illustrating that our different classes of objects largely overlap in this diagram.

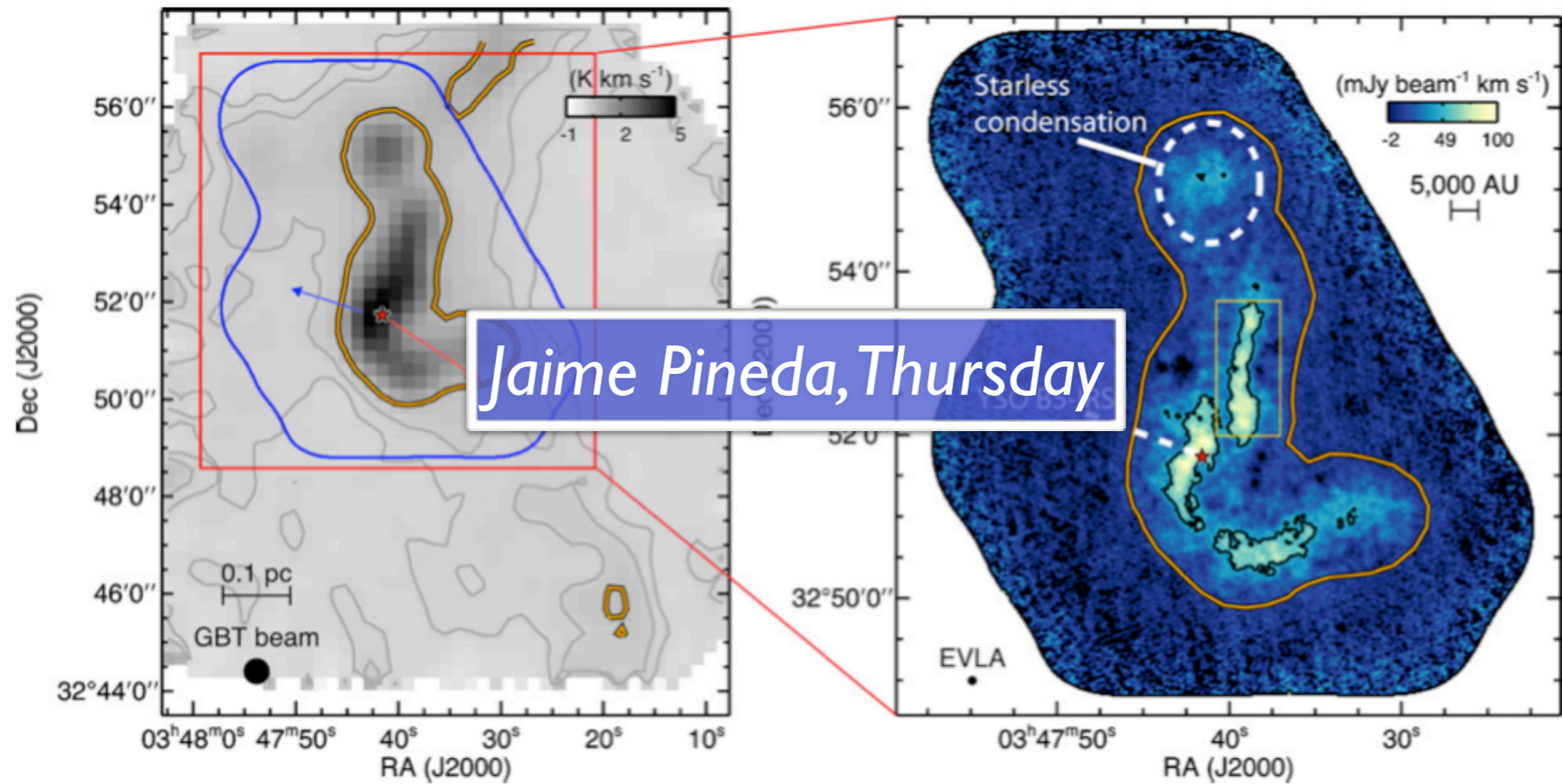
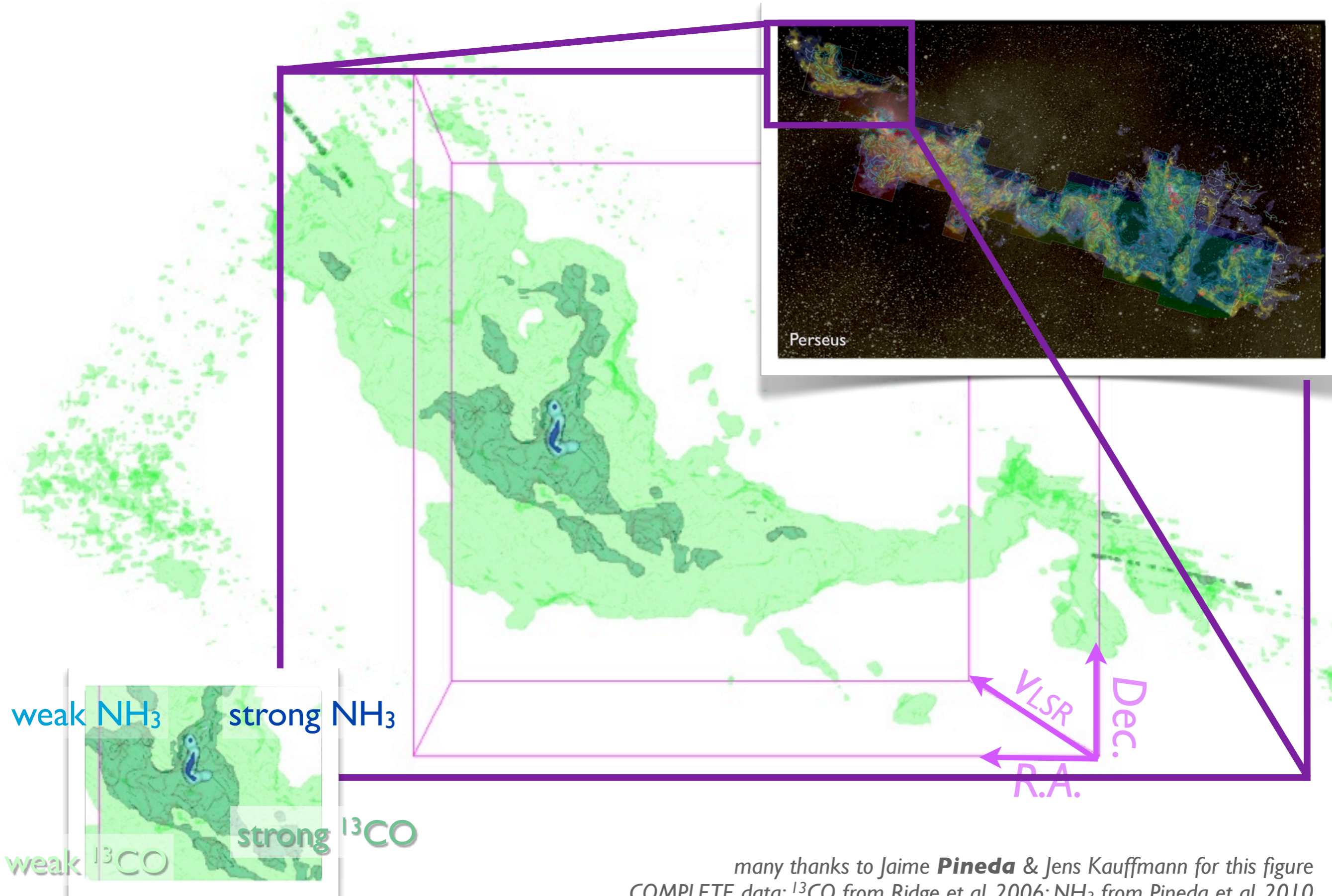


Figure 1. Left panel: integrated intensity map of B5 in NH_3 (1,1) obtained with GBT. Gray contours show the 0.15 and 0.3 K km s^{-1} level in NH_3 (1,1) integrated intensity. The orange contours show the region in the GBT data where the non-thermal velocity dispersion is subsonic. The young star, B5-IRS1, is shown by the star in both panels. The outflow direction is shown by the arrows. The blue contour shows the area observed with the EVLA and the red box shows the area shown in the right panel. Right panel: integrated intensity map of B5 in NH_3 (1,1) obtained combining the EVLA and GBT data. Black contour shows the 50 $\text{mJy beam}^{-1} \text{ km s}^{-1}$ level in NH_3 (1,1) integrated intensity. The yellow box shows the region used in Figure 4. The northern starless condensation is shown by the dashed circle.

Pineda et al. 2010, 2011

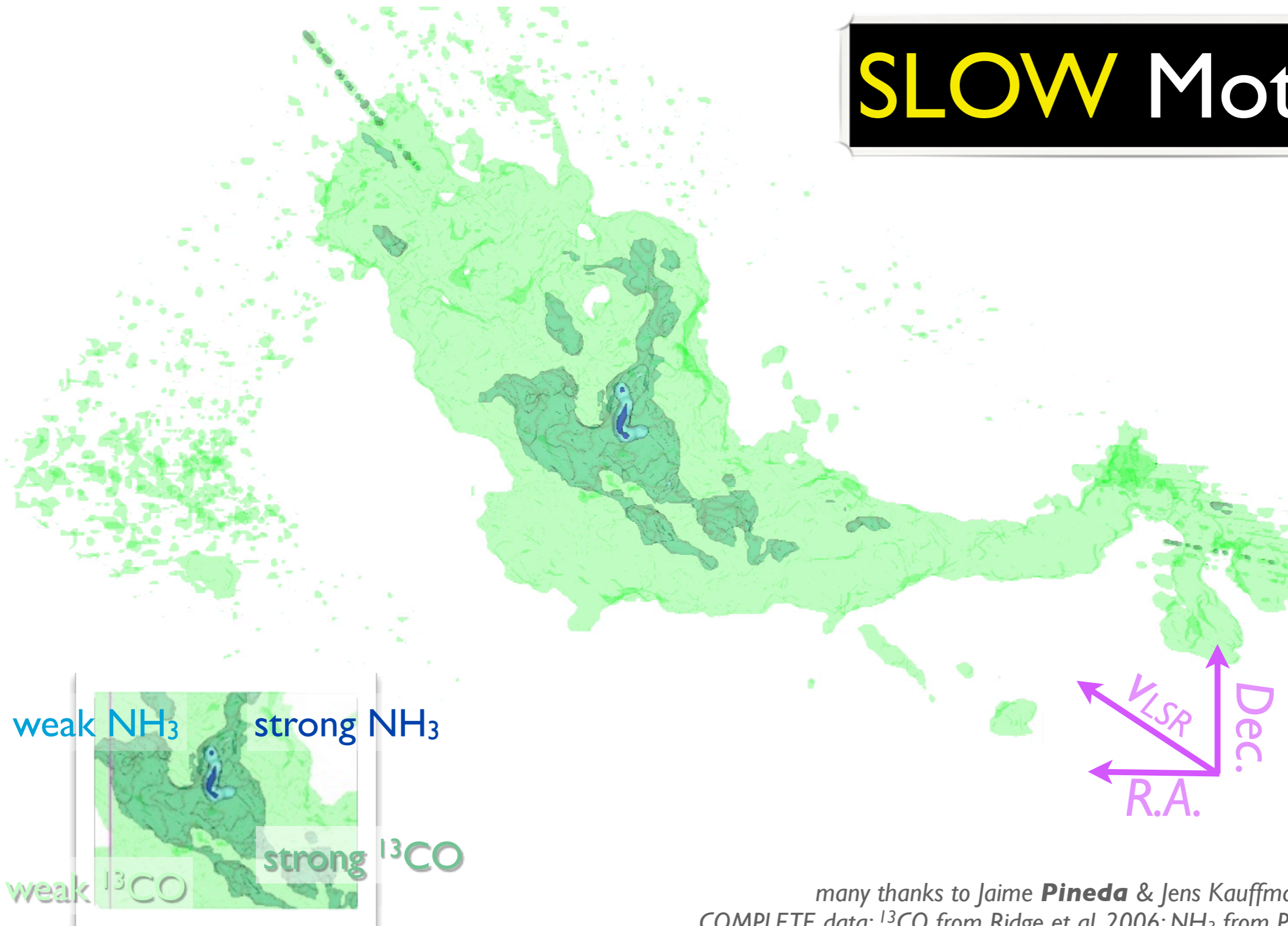
(*p-p-v* structure of the) B5 region in Perseus



many thanks to Jaime **Pineda** & Jens Kauffmann for this figure
COMPLETE data: ^{13}CO from Ridge et al. 2006; NH_3 from Pineda et al. 2010

(*p-p-v* structure of the) B5 region in Perseus

SLOW Motion

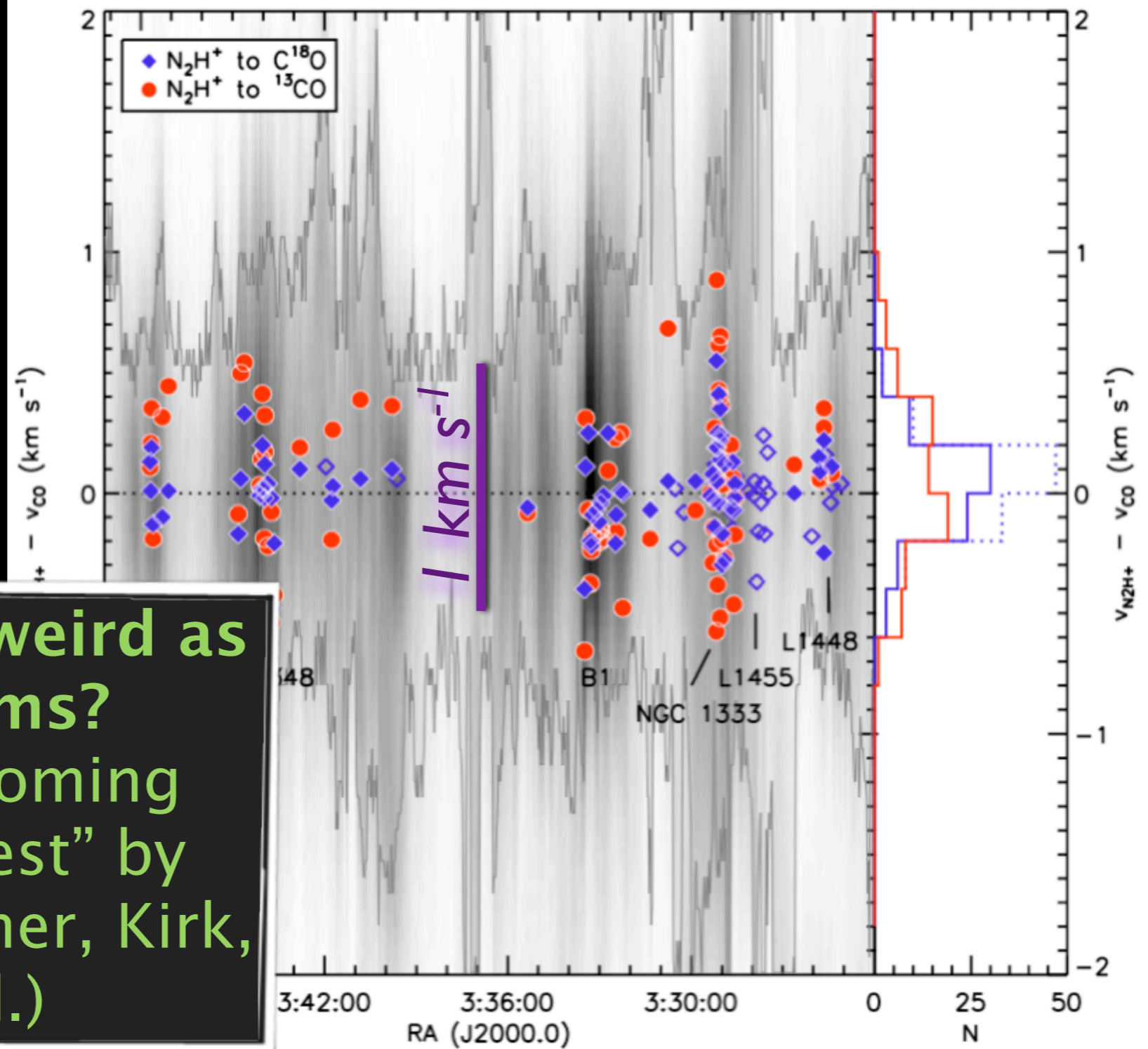


many thanks to Jaime **Pineda** & Jens Kauffmann for this figure
COMPLETE data: ^{13}CO from Ridge et al. 2006; NH_3 from Pineda et al. 2010

SLOW Motion

of cores with respect to clouds
of young stars with respect to cores

Is this as weird as
it seems?
(See upcoming
“Taste Test” by
Harris, Offner, Kirk,
et al.)



SLOW Motion

of cores with respect to clouds
of young stars with respect to cores

- YSO
- ◆ SCUBA core
- $1 M_{\odot} \text{pc}^{-3}$
- $25 M_{\odot} \text{pc}^{-3}$

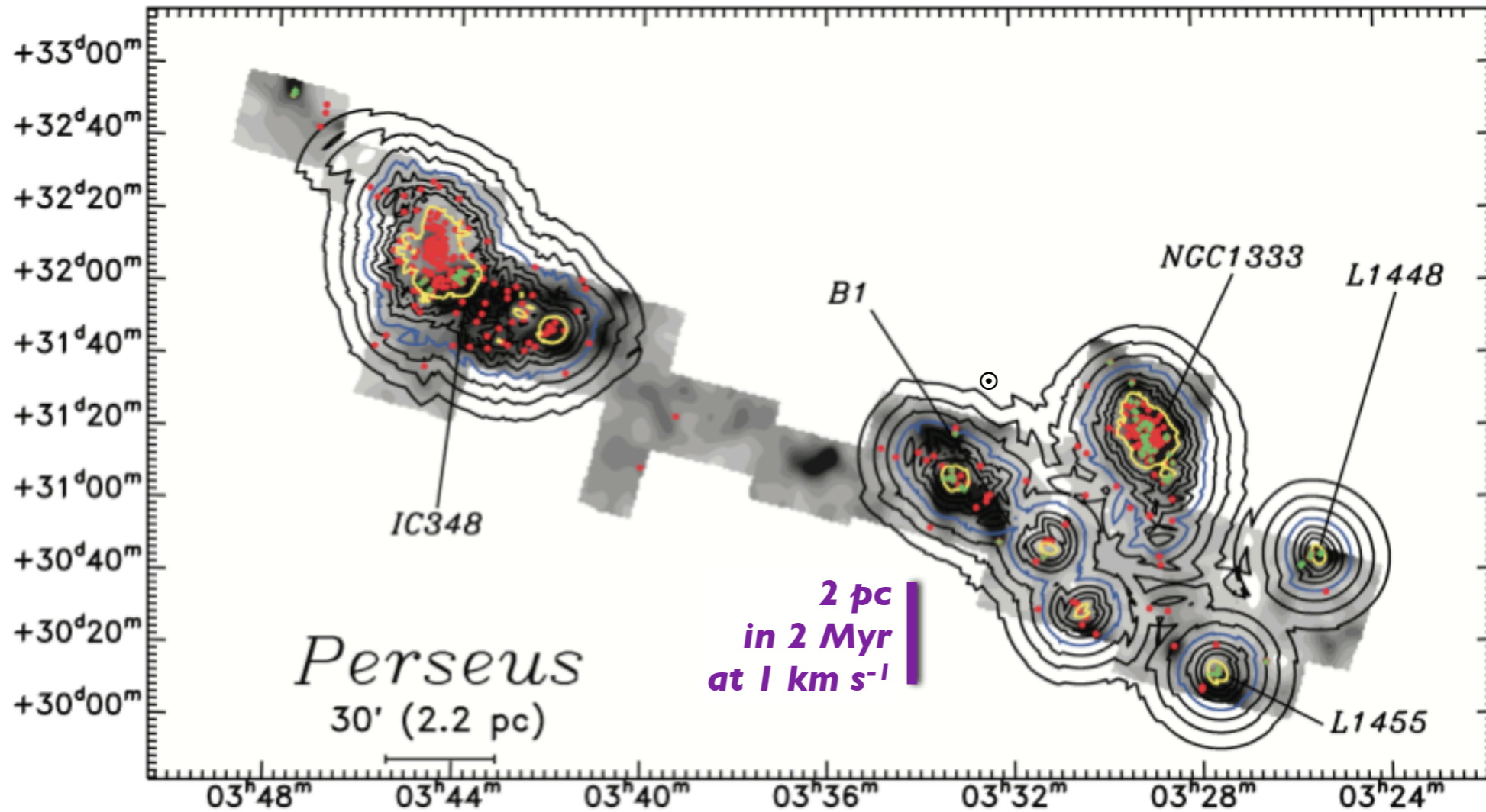


FIG. 13.— Volume density contours of the YSOs in Ophiuchus (*top panel*), Perseus (*bottom panel*) shown on top of extinction maps (*gray-scale*) based on the c2d data (Evans et al. 2007). In both panels the black contours indicate the volume densities corresponding to 0.125, 0.25, 0.50, 2.0, and 4.0 $M_{\odot} \text{pc}^{-3}$. The blue contours show volume densities of $1 M_{\odot} \text{pc}^{-3}$, corresponding to the criterion ($1 \times \text{LL03}$ in the text) for identifying clusters suggested by Lada & Lada (2003) and the yellow contours to volume densities of $25 M_{\odot} \text{pc}^{-3}$ ($25 \times \text{LL03}$ in the text). The red dots show the locations of the YSOs and the green plus signs the locations of the SCUBA cores in the two clouds.

Value of Open Access to Large Data Sets

Yes, I do mean you...

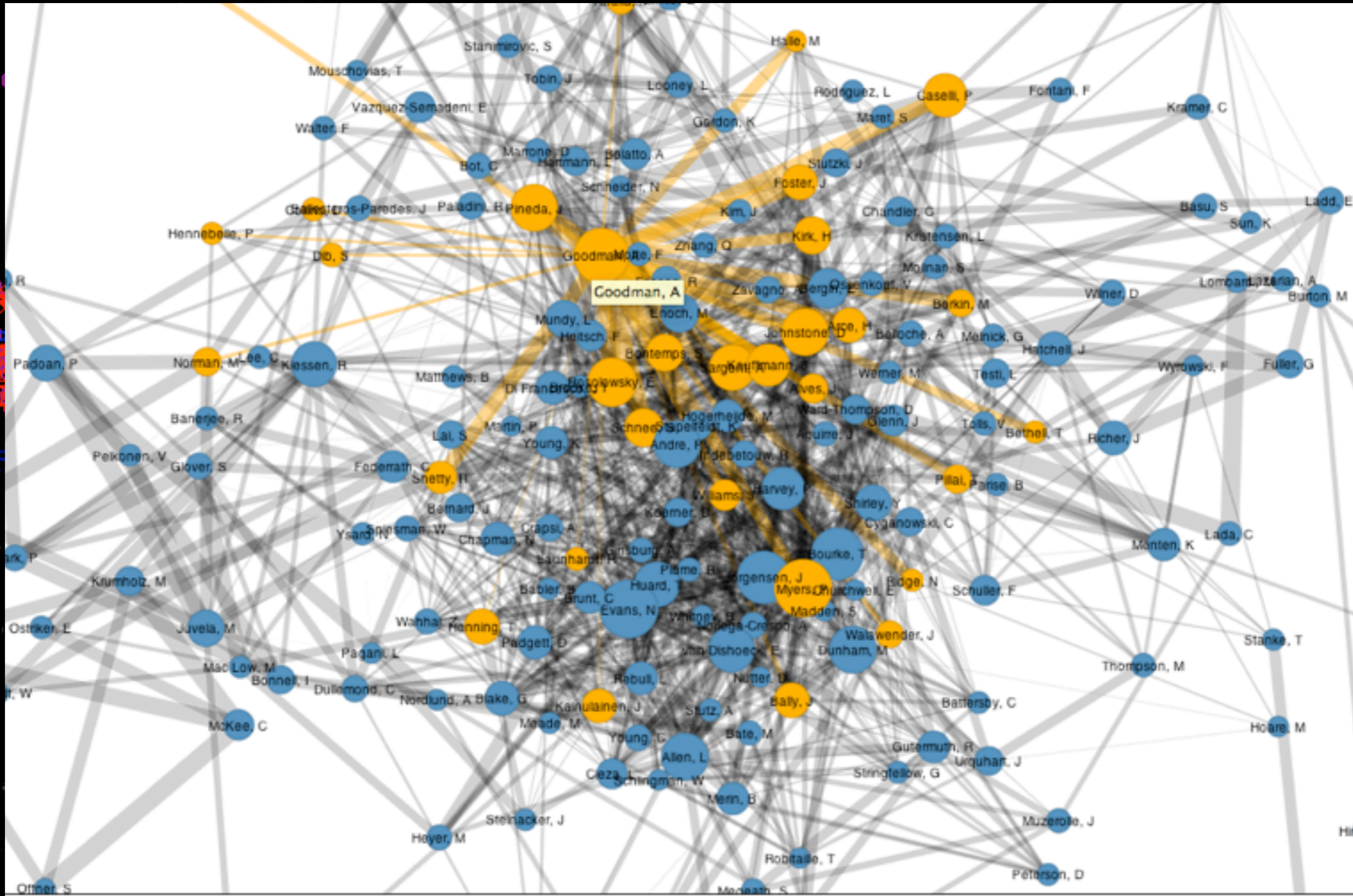
COMPLETE

~900 citations,
10% to data paper...
H-index of 17,
normalized H-index=
(17 papers) /
(5 years since data paper)
= 3.5!

The screenshot shows the 'Herschel Science Archive' web interface. At the top, there's a navigation bar with 'esa' logo and 'Herschel Science Archive' text. Below it are tabs for 'Query Specification', 'Latest Results', 'Shopping Basket', 'Login/Register', 'Logout', and 'On-demand Monitor'. The main content area is titled 'Query Specification' and includes a 'Query Specification' button, 'Execute Query', 'Cancel Query', and 'View/Edit SQL' buttons. There are also 'Sort Criteria' and 'Sort Order' dropdowns. The 'Principal Search Criteria' section has fields for 'Observation ID', 'Proprietary status', 'Search Target By' (Name, Equatorial, Galactic, Ecliptic), 'Name' (for SIMBAD), 'Radius', 'Instrument', and 'Obs Type' (Standard Data). Below this are four instrument-specific filter boxes: 'All | HIFI | None' (Single Point, Mapping, Spectral Scan), 'All | PACS | None' (Pacs Photometer, Range Spectroscopy, Line Spectroscopy), 'All | SPIRE | None' (Photometer, Spectrometer), and 'All | SPIRE PACS | None' (Parallel Mode). The 'Proposal' section has fields for 'Observer', 'Proposal ID', and 'AOR label'. At the bottom, there's a 'Timing Constraints' section.



Note: I own “universe3d.org”—let me know if you’d like to contribute.



YELLOW?

(What I've learned...)

Tell me more...



- ★ “Column Temperature”
- ★ ^{13}CO poor tracer of column density, abundance not the problem
- ★ “lognormal” (*but...*)
- ★ “Cloudshine”
- ★ GNICEST (and CS!)
- ★ virial theorem over-used?
- ★ Dangers of p - p - v “observer” space
- ★ Perils of CLUMPFIND
- ★ Benefits of Dendrograms
- ★ Value of *Tasting Dust & b-T*
- ★ Spherical(!) Outflows
- ★ Cores in/out of Clusters NOT so Different
- ★ Coherent Cores are Real, and they Fragment (into filaments!)
- ★ SLOW motion of cores & stars w.r.t. environs
- ★ Density “thresholds” more complicated than you think
- ★ Open Access is GOOD

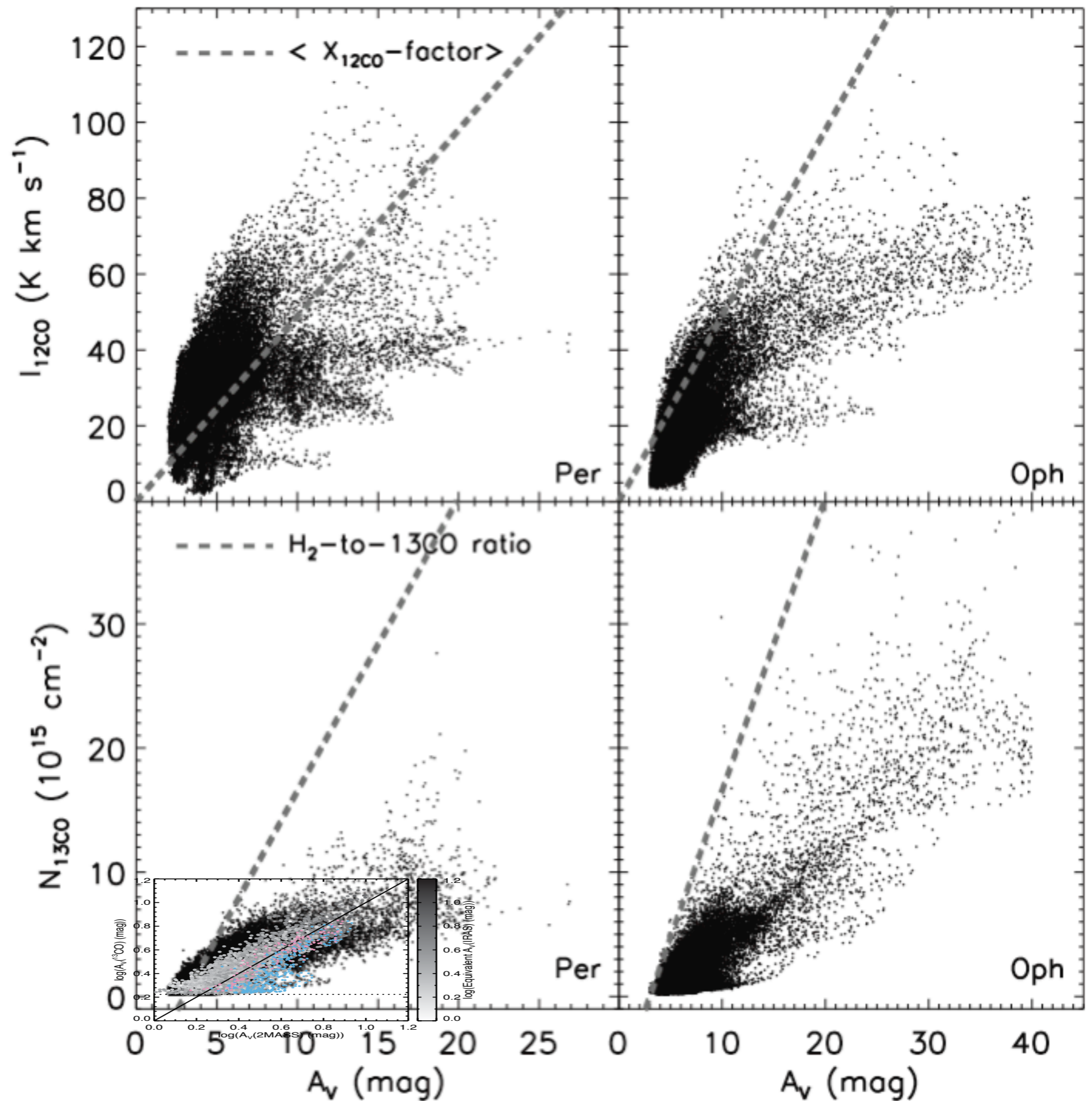
Caselli

Pineda

Kauffmann

Heiderman

FYI:
Going
Deeper...



Heiderman et al. 2010;
cf. Pineda et al. 2008